Electronic Supplementary Material (ESI) for ChemComm.

An internal electron reservoir enhances catalytic CO_2 reduction by a semisynthetic enzyme

Camille R. Schneider and Hannah S. Shafaat

Electronic Supporting Information
Table of Contents

Materials and Methods

All materials and reagents were used as received unless specifically noted.

Sequencing data

All Az mutants (sequences below) were heterologously expressed using standard techniques. The pUC18 plasmid containing the *Pseudomonas aeruginosa (Pae*) wild-type (WT) Az gene was generously donated by Professor Judy Kim (UCSD). H83Q/Q107H Az was created using the following mutagenic primers (Sigma Aldrich):

`5′-CGAGTTATCGCCCAGACCAAGCT-3′` (H83Q forward)
`5′-CAGCTTGGTCTGGGCGATAACTC-3′` (H83Q reverse)
`5′-AAAGAAGGTGAACATTACATGTTC-3′` (Q107H forward)
`5′-GAACATGTAATGTCACCTTCTT-3′` (Q107H reverse)

H83Q/Q107H Az DNA sequence:

GCT GAA TGC TCC GTT GAT ATC CAG GGT AAT GAT CAG
ATG CAG TTC AAC ACC AAC GCC ATC ACC GTC GAC AAG
AGC TGC AAG CAG TTC ACT GTT AAC CTG
TCT CAC CCA GGT AAC CTG CCG AAG AAC GTT ATG GGT
CAC AAC TGG GTT CTG TCC ACC GCG GCT GAC ATG CAA
GGC GTT GTC ACT GAC GGT ATG GCT AGC GGT CTG GAT
AAA GAC TAC CTG AAG CCG GAT GAC
TCT CGA GTT ATC GCC **CAG** ACC AAG CTG ATC GGA TCC
GGT GAA AAA GAC TCC GTT ACT TTC GAC GTT TCC AAG
CTT AAA GAA GGT GAA **CAT** TAC ATG TTC
TTC TGC ACT TTC CCG GGT CAC TCC GCA CTG ATG AAA
GGT ACC CTG ACT CTG AAA TAG

H83Q/Q107H Az amino acid sequence:

AECSVDIQGNDQMQFNTNAITVDKSCKQFTVNLSHPGNLPKNVMGHNWVLSTAADMQGVVTD
GMASGLDKDYLKPDDSRVIA**Q**TKLIGSGEKDSVTFDVSKLKEGE**H**YMFFCTFPGHSALMKGTL
TLK*

Wild-type Az DNA sequence:

GCT GAA TGC TCC GTT GAT ATC CAG GGT AAT GAT CAG
ATG CAG TTC AAC ACC AAC GCC ATC ACC GTC GAC AAG
AGC TGC AAG CAG TTC ACT GTT AAC CTG
TCT CAC CCA GGT AAC CTG CCG AAG AAC GTT ATG GGT
CAC AAC TGG GTT CTG TCC ACC GCG GCT GAC ATG CAA
GGC GTT GTC ACT GAC GGT ATG GCT AGC GGT CTG GAT
AAA GAC TAC CTG AAG CCG GAT GAC
TCT CGA GTT ATC GCC **CAC** ACC AAG CTG ATC GGA TCC
GGT GAA AAA GAC TCC GTT ACT TTC GAC GTT TCC AAG
CTT AAA GAA GGT GAA **CAG** TAC ATG TTC
TTC TGC ACT TTC CCG GGT CAC TCC GCA CTG ATG AAA
GGT ACC CTG ACT CTG AAA TAG

Wild-type Az amino acid sequence:

AECSVDIQGNDQMQFNTNAITVDKSCKQFTVNLSHPGNLPKNVMGHNWVLSTAADMQGVVTD
GMASGLDKDYLKPDDSRVIA**H**TKLIGSGEKDSVTFDVSKLKEGE**Q**YMFFCTFPGHSALMKGTL
TLK*

Azurin expression and purification

Sequence confirmed plasmids were transformed into *E. coli* BL21-DE3* competent expression cells (Life Technologies). Mutant and WT Az were expressed and purified using similar protocols, slightly modified from prior reports.[1] Briefly, a starter growth using Luria broth (LB) media (BioBasic) containing 70 mg/L carbenicillin (GoldBio Technologies) was shaken at 200 rpm for 14 hours at 37°C. The starter growth was then divided into 1 L flasks of LB with 70 mg/mL carbenicillin and grown to an OD_{600} of 1. Cells were induced with 1 mM IPTG (GoldBio Technologies) and shaken at 200 rpm for 14 hours at 18°C.

After induction, the cells were pelleted *via* multiple rounds of centrifugation at 5600 x *g* (Avanti J-E centrifuge, JLA-10.500 rotor), and the resultant cell pellets were washed twice with 20 mM Tris, pH 7.8, and stored at -80°C until needed. Pellets were lysed at room temperature using 1 mg/g lysate of egg white lysozyme (GoldBio Technologies) and 0.1 mg/g lysate DNase (GoldBio Technologies) in 20 mM phosphate, pH 7.6 buffer, for 90 minutes. The lysate was centrifuged at 39,000 x *g* to remove cellular debris. The resultant supernatant was treated with 1 M sodium acetate, pH 4.5, to bring the lysate solution to pH 5, causing formation of white precipitate. Following another round of centrifugation, excess $Cu^{II}SO_4$ was added to the supernatant. After a final centrifugation, the lysate was dialyzed overnight against 1 mM sodium acetate, pH 4.5. All centrifugation steps were carried out at 4°C.

CuAz was purified on a 5-mL, self-packed Source 15S cation exchange column (GE Amersham). CuAz was eluted around 50% eluent using a 1 - 300 mM salt gradient with sodium acetate, pH 4.5. Az purity was assessed both spectroscopically and by SDS gel electrophoresis. Under denaturing conditions, Az runs as a monomer of ~14 kDa (Fig. S15). Fractions were additionally assessed for purity using the A_{628}/A_{280} ratio of at least 0.5 for CuAz.[2] Fractions observed to be pure by gel electrophoresis but showing a spectroscopic ratio of less than 0.5 were attributed to ZnAz contamination.

Az metal extraction and reconstitution

All Az variants were subjected to metal extraction and reconstitution following published protocols.[1,3,4] CuAz was reduced with an excess of sodium dithionite (Acros Organics) and dialyzed for three, 4-hour rounds against a solution of 400 mM potassium cyanide (Alfa Aesar), buffered in 100 mM potassium phosphate at pH 8.0, to generate apo-Az. To remove excess cyanide, apo-Az was then dialyzed against 100 mM potassium phosphate, pH 8.0, for three, 4-hour rounds. Excess phosphate was removed by dialyzing against 10 mM Tris, pH 7.4 for 4 hours. Metal reconstitution was achieved by overnight dialysis against 7.5 mM $Cu^{II}SO_4$ or $Zn^{II}SO_4$ in 50 mM Tris, pH 7.4. Excess metal was removed by dialysis against 50 mM Tris, pH 7.4. Metal incorporation was verified using absorption spectroscopy (Figs. S16 and S17).

Az-[1] generation

$[Ni(cyclam)]^{2+}$, ([1], cyclam = 1,4,8,11-tetraazacyclotetradecane) was synthesized following a published protocol.[5] Cyclam (Acros Organics) was dissolved in ethanol and combined in a 1:1 mole ratio with $Ni^{II}Cl_2$. The resulting mauve solution was heated slightly and stirred for 15 minutes. $[1]Cl_2$ was precipitated upon the addition of diethyl ether and collected by vacuum filtration. Pure Az variants were concentrated and buffer exchanged into 50 mM CHES buffer, pH 9.0, using centrifugal filter devices (Millipore Centricons, MWCO 3.5 kDa). To generate Az-[1] hybrids, Az was shaken at 70 rpm for 48 hours, at 37°C, with a ten-fold molar excess of [1] in 50 mM CHES, pH 9.0. Excess [1] was removed via a PD-10 desalting column (Bio Rad) immediately prior to use.

UV-Vis spectroscopy

All UV-visible absorption spectra were collected on a Shimadzu UV-2600 spectrophotometer.

Electrochemistry experiments

All cyclic voltammetry (CV) electrochemistry experiments were conducted using a WaveNow potentiostat (Pine Instruments). Experiments requiring an inert atmosphere were performed in a glovebox (Vigor Technologies) under a nitrogen atmosphere. For experiments requiring CO_2, buffers were extensively sparged before use with a high purity carbon dioxide gas cylinder (Praxair) and experiments conducted under a saturated CO_2 atmosphere. A typical three-electrode set up was employed for solution-phase electrochemistry, with a 3 mm glassy carbon working electrode (CH Instruments), a platinum wire counter electrode, and a mini saturated Ag/AgCl reference electrode (Pine Instruments). Prior to each experiment, the glassy carbon working electrode was polished for 60 seconds with 1.0 micron alumina powder, rinsed with deionized water, and polished with 0.05 micron alumina powder. The electrode was rinsed again and sonicated for three minutes prior to use. All potentials were reported against NHE by the addition of +198 mV to the experimentally measured potentials. To account for the acidity of dissolved CO_2, experiments in saturated CO_2 solution were carried out in a mixed buffer system, consisting of 10 mM CHES, pH 9.0, 40 mM phosphate, pH 7.0, and 80 mM KCl as the supporting electrolyte. Following the CO_2 sparge, the final pH of this buffer mixture was typically 6.1. For experiments performed in the absence of CO_2, the pH of the buffer mixture was adjusted as necessary to pH 6.1.

Electrochemistry data analysis

Three cyclic voltammograms were averaged to give the final reported CVs. Any baseline-subtracted figures were corrected using the QSOAS program.[6] To determine the reported onset potentials for catalysis, the cathodic segments for each variant were averaged. For $[Ni(cyclam)]^{2+}$, which displayed typical electrocatalytic signals, the E_p for catalysis was defined as the point at which the curvature of the cathodic catalytic wave of the CV was maximized. This was found by taking the derivative of the cathodic wave and identifying its peak position (Figure S6, inset). As mentioned in the main text, an analogous procedure could not be performed for the Az-[1] variants, which all displayed non-ideal electrocatalytic behavior likely due to slow diffusion and interfacial electron transfer. Thus, the onset potentials listed for the protein variants were defined as the potential at which the catalytic current matched that of free [1] at E_p (Table S1 and Fig. S6). By carrying out this analysis, direct comparison of the onset potentials for each of the systems was possible.

$[Ru^{II}(bpy)_3]^{2+}$ photoassay

The experimental conditions for the $[Ru^{II}(bpy)_3]^{2+}$ assay were adapted from a previously published protocol.[7] All assays were performed on ice in a mixed buffer system of 10 mM CHES, pH 9.0, 800 mM phosphate, pH 7.2 (final pH typically 7.05), under a CO_2 atmosphere. A strong dependence of activity on the Az-[1] stock concentration was observed; as such, protein-[1] stocks at 50 μM concentration were diluted for assays. Each assay contained 4 μM catalyst, 1 mM $[Ru(bpy)_3]^{2+}$ (Sigma Aldrich), and 100 mM ascorbate (Ricca Chemical), unless otherwise noted. For photoexcitation, four LUXEON Rebel ES LEDs (447.5 nm) were spaced symmetrically, 10 cm from the septa-capped vial, giving a measured power of 4.5 mW at the sample. At the specified timepoints, 250 μL gas samples were removed from the headspace and injected into the gas chromatograph for analysis.

Gas chromatography analysis

Gas chromatography analysis was performed using a Shimadzu GC-2014 fuel cell analyzer system, which is equipped with both a thermal conductivity detector and a flame ionization

detector. For each experimental timepoint, 250 µL injections were taken from the sample headspace. Hydrogen production was quantified using a thermal conductivity detector, while CO production was quantified using a flame ionization detector coupled to a methanizer. Argon was used as the carrier gas for all experiments. Separation was achieved with the use of the following columns: HayeSep-N (3 m, 80/100 mesh), HayeSep-T (2 m, 80/100 mesh), Shimalite Q (0.2 m, 100/180), Shimalite Q (0.25 m, 100/180), Shimalite Q (0.15 m, 100/180), and a 5 Ångstrom molecular sieve (2.5 m, 60/80). Standard curves for quantitative analysis of gas were carried out using varying size injections (50 µL – 2.5 mL) of Scotty standard gas calibration mixture (Fig. S22).

Mass spectrometry analysis

All MALDI-TOF samples were prepared on a ground steel plate (Bruker MSP 96 microScout Target). A final concentration of 10 µM protein was used for analysis. The matrix was composed of 200 mM sinapic acid (Sigma-Aldrich) in 30 mM ammonium citrate and 30 % acetonitrile. The sample/matrix mixture was allowed to dry on the plate overnight prior to analysis. Samples were analyzed on a Bruker microFlex MALDI-TOF spectrometer (Fig. S24).

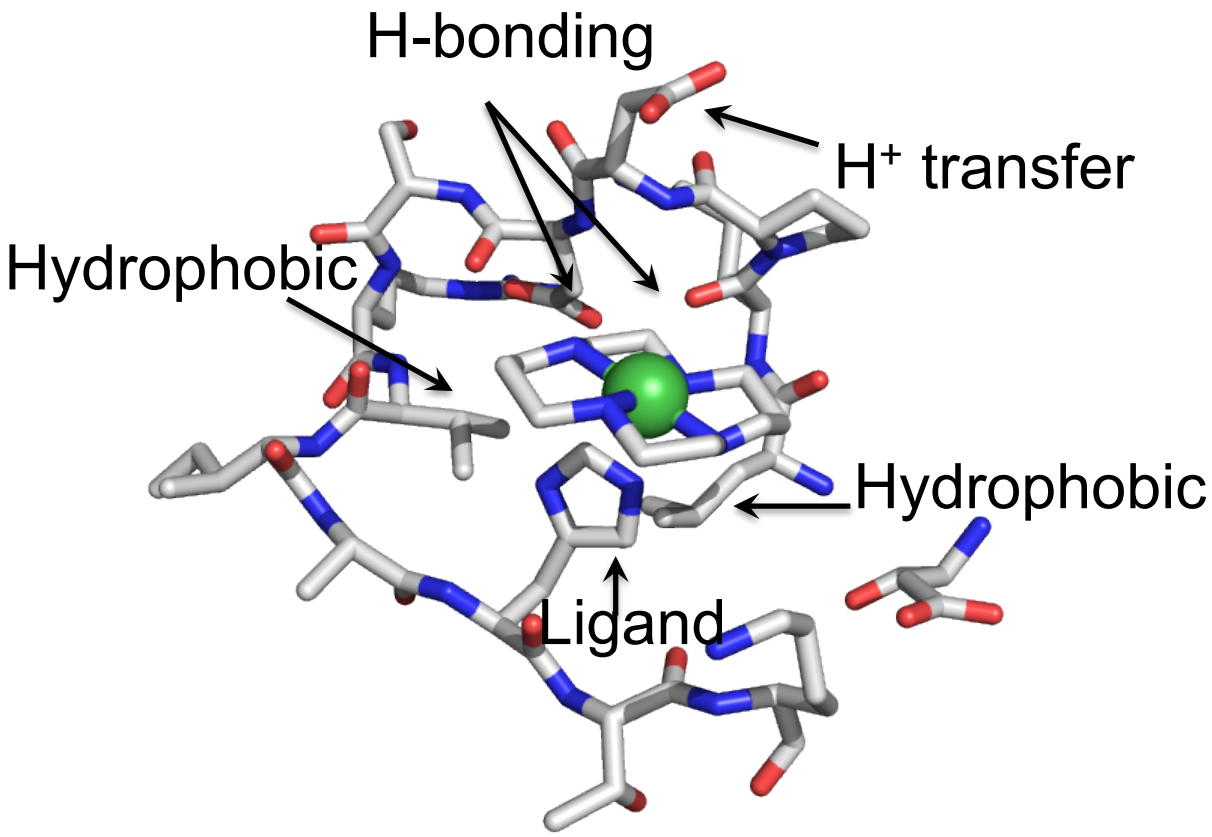

Figure S1. (PDB ID: 4AZU) Putative secondary coordination sphere interactions around His83-coordinated [1].

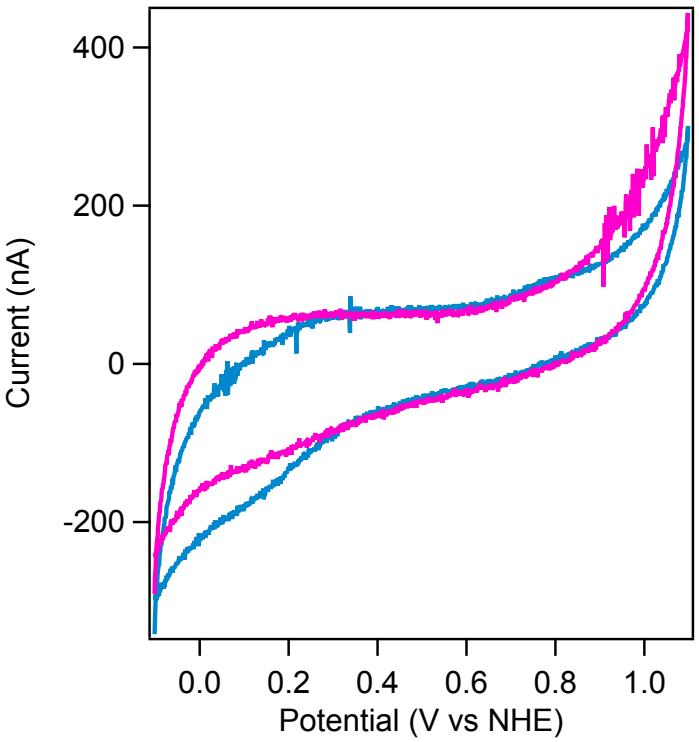

Figure S2. Cyclic voltammograms of 150 μM H83Q ZnAz (pink) and H83Q CuAz (turquoise) after incubation with 10-fold excess [1] and desalting. Measurements were carried out under a CO_2 atmosphere with a glassy carbon working electrode in a 10 mM CHES, 40 mM phosphate mixed buffer system at pH 6.1 containing 80 mM KCl (T = 20 ˚C, ν = 50 mV/s). Potentials were measured against an Ag/AgCl reference electrode and converted to NHE by the addition of +198 mV.

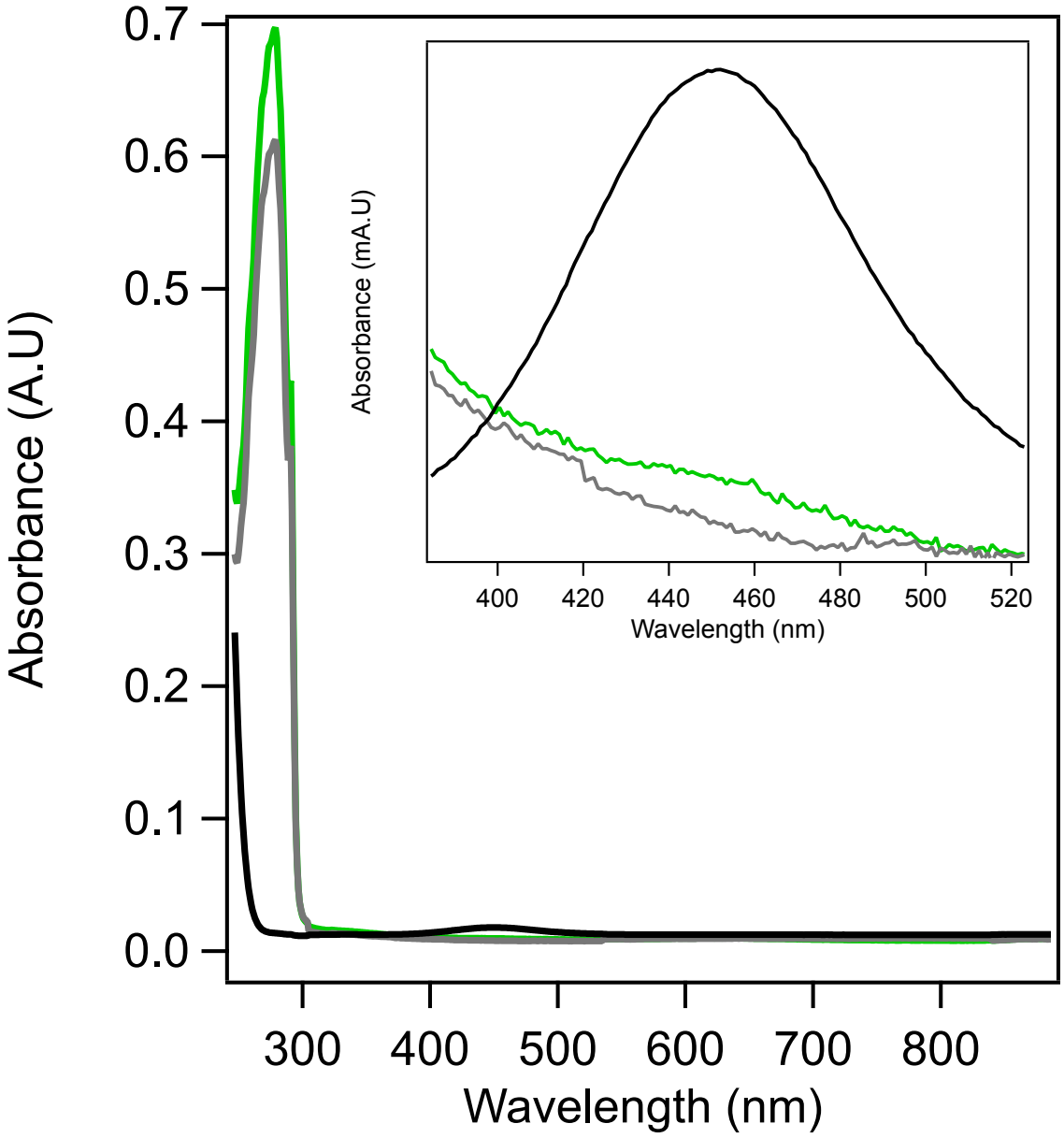

Figure S3. Absorption spectra of 60 μM H83Q/Q107H ZnAz (gray), 65 μM H83Q/Q107H ZnAz-[1] (green) and 1 mM free [1] (black) in 50 mM CHES buffer, pH 9.0, following desalting on a PD-10 column. (*Inset*) Enlarged spectra around region of interest showing absorption features of [1]. Spectrum reflects a ~40% labeling efficiency (65 μM total protein with 24 μM [1]).

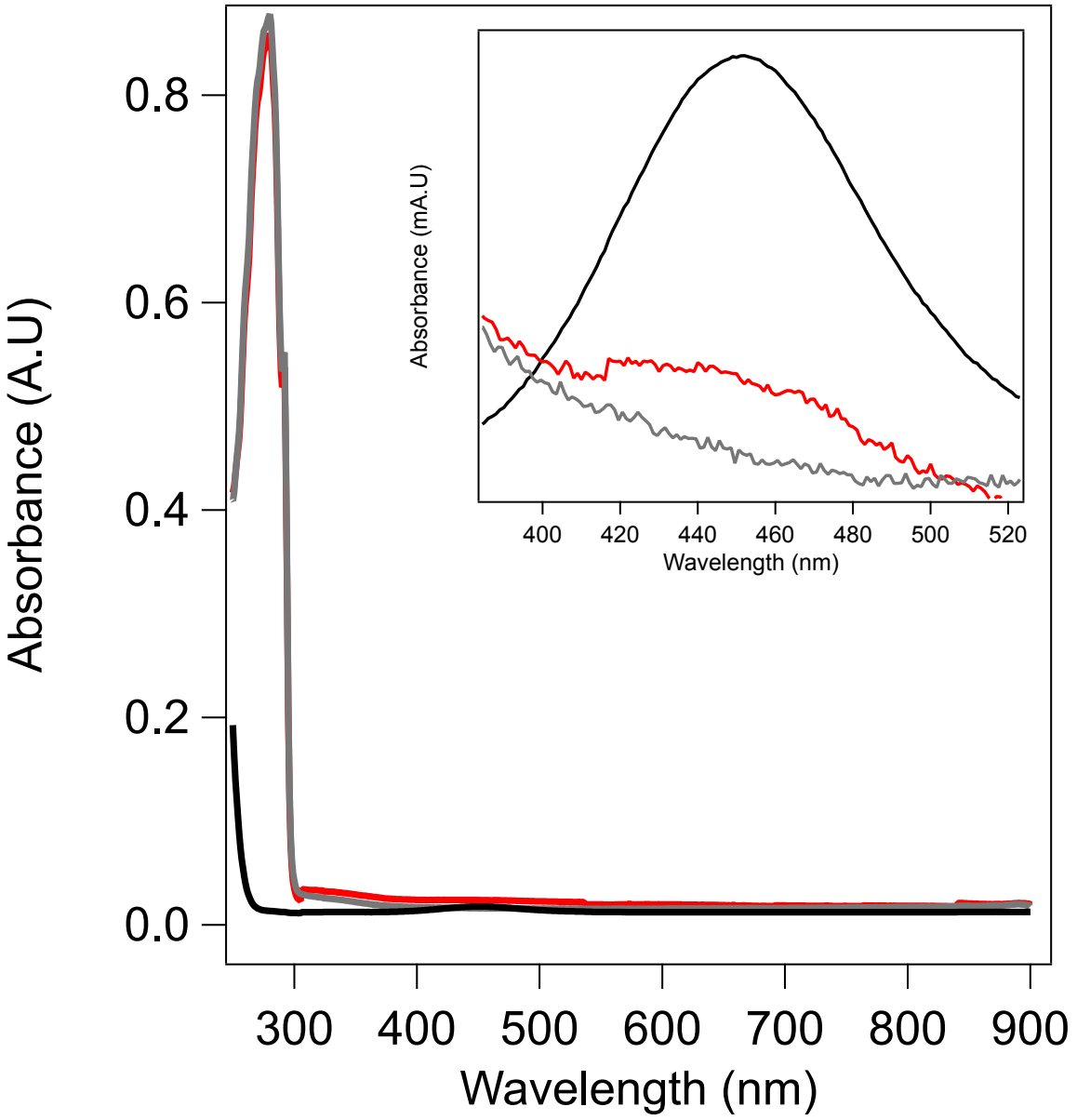

Figure S4. Absorption spectra of 80 μM WT ZnAz (gray), 80 μM WT ZnAz-[1] (green) and 1 mM free [1] (black) in 50 mM CHES buffer, pH 9.0, following desalting on a PD-10 column. (*Inset*) Enlarged spectra around region of interest showing absorption features of [1]. Spectrum reflects a ~40% labeling efficiency (80 μM total protein with 30 μM [1]).

Protein variant	E° ($Ni^{III/II}$) (mV vs. NHE) [ΔE_{pk-pk} (mV)]	$E_{cat,\ onset}$ (V vs. NHE)	Corrected TON	TOF ($hour^{-1}$)	Selectivity ratio (CO/H_2)
H83Q/Q107H CuAz-[1]	715 [95]	-1.10	37	12.5	0.6
H83Q/Q107H ZnAz-[1]	695 [85]	-1.30	14.6	5.8	0.7
WT CuAz-[1]	705 [80]	-1.23	34	13.7	1.9
WT ZnAz-[1]	680 [60]	-1.35	14.5	5.8	3.5
$[Ni^{II}(cyclam)]^{2+}$	690 [60]	-1.20	14.5	5.5	0.2

Table S1. Tabulated electrochemical and catalytic parameters for [1]-labeled azurin variants in comparison to free [1] in solution. TON was calculated for the assay after 5 hours total irradiation; TOF was calculated using the first two hours of catalysis. TON and TOF were calculated assuming a 40% labeling efficiency. Selectivity ratio (CO/H_2) is given after twenty minutes of irradiation during $[Ru(bpy)_3]^{2+}$ photoassays.

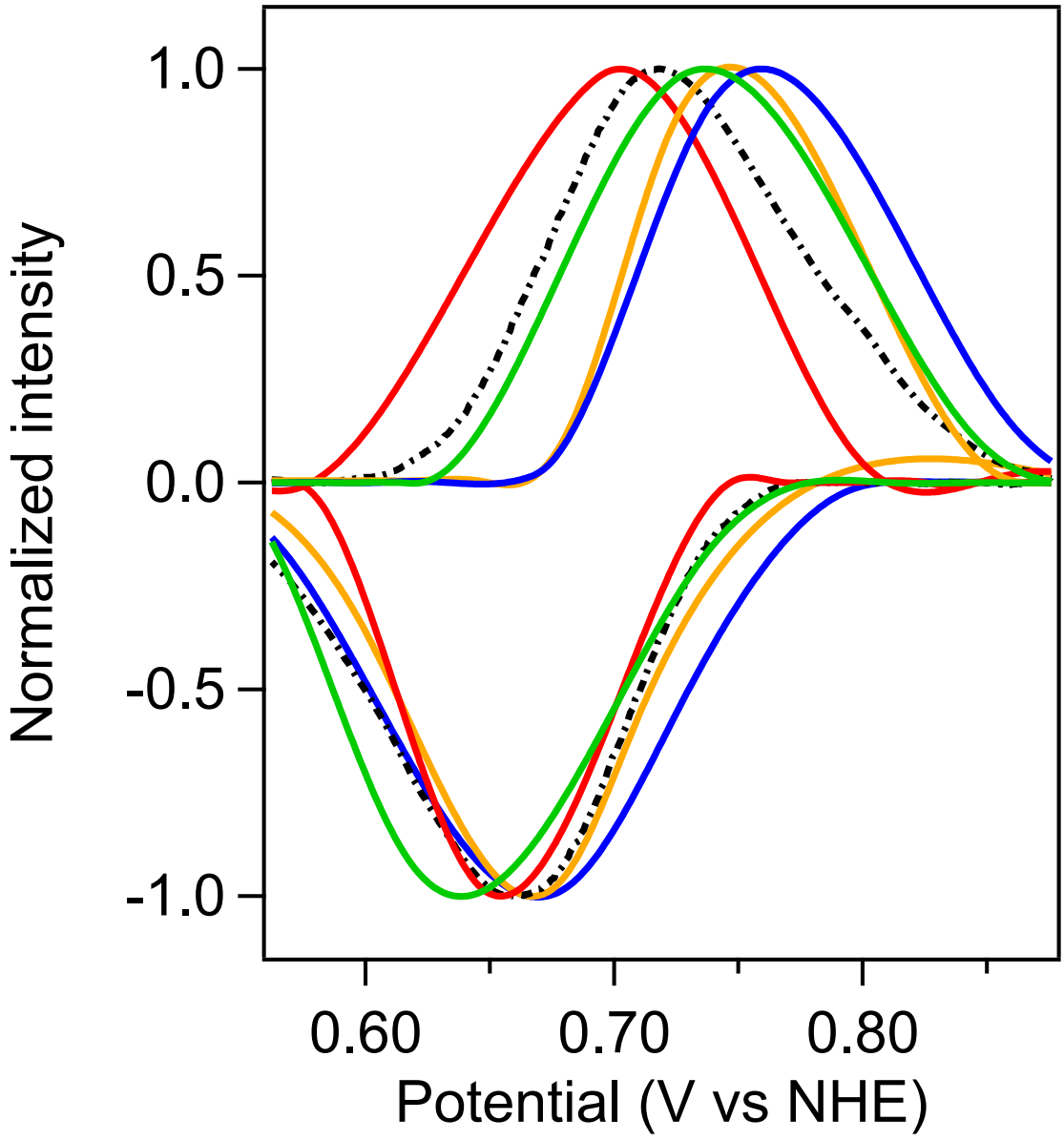

Figure S5. Baseline-corrected, normalized cyclic voltammogram data at the $Ni^{III/II}$ redox couple of H83Q/Q107H CuAz-[1] (blue), H83Q/Q107H ZnAz-[1] (green), WT ZnAz-[1] (red), WT CuAz-[1] (orange) in comparison to free [1] in solution (dot-dashed black). Baseline subtractions and filtering were performed in QSOAS. Measurements were carried out under a CO_2 atmosphere with a glassy carbon working electrode in a 10 mM CHES, 40 mM phosphate mixed buffer system at pH 6.1 containing 80 mM KCl (T = 20 ˚C, ν = 10 mV/s). Potentials were measured against an Ag/AgCl reference electrode.

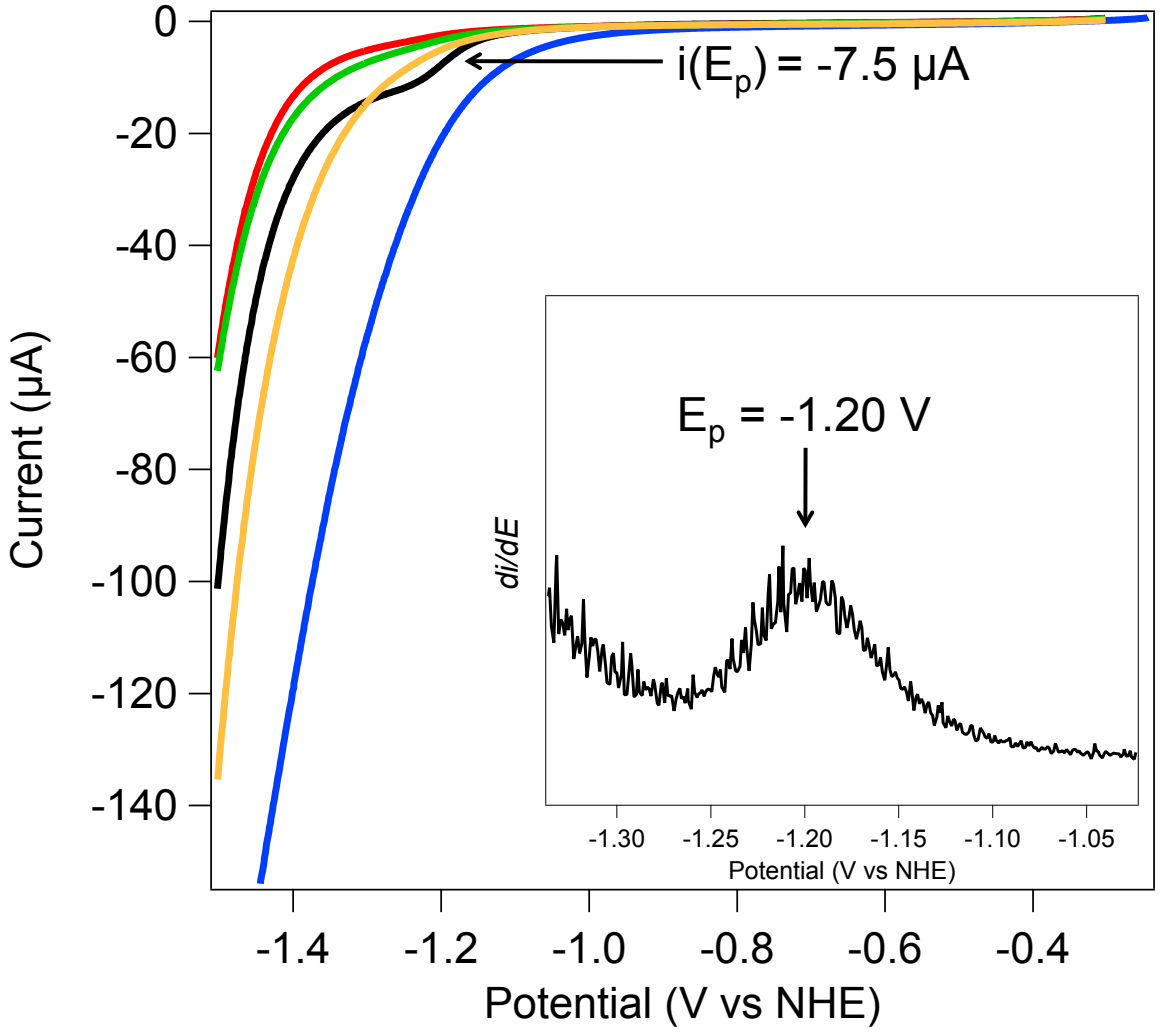

Figure S6. Averaged cathodic segments of H83Q/Q107H CuAz-[1] (blue), H83Q/Q107H ZnAz-[1] (green), WT ZnAz-[1] (red), WT CuAz-[1] (orange) in comparison to free [1] in solution (black). (*Inset*) First derivative of the CV of [1], used to determine the value of E_p. Measurements were carried out under a CO_2 atmosphere with a glassy carbon working electrode in a 10 mM CHES, 40 mM phosphate mixed buffer system at pH 6.1 containing 80 mM KCl (T = 20 ˚C, ν = 50 mV/s). . Potentials were measured against an Ag/AgCl reference electrode and converted to NHE by the addition of +198 mV.

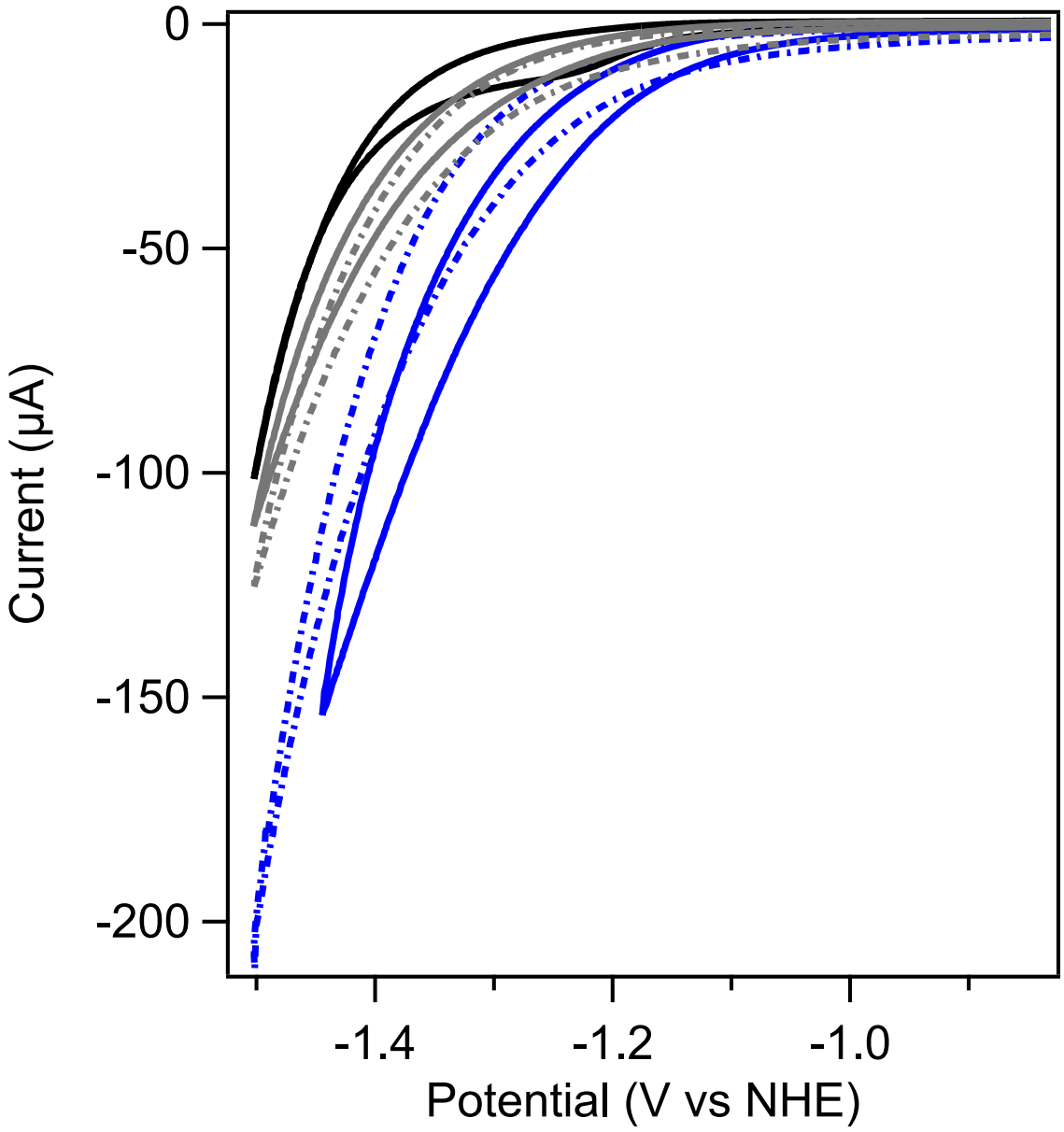

Figure S7. Cyclic voltammograms of H83Q/Q107H CuAz-[1] (blue), H83Q/Q107H CuAz (gray), and free [1] in solution (black) under CO_2-saturated (solid lines) and inert (dotted lines) atmospheres. Measurements were carried out with a glassy carbon working electrode in a 10 mM CHES, 40 mM phosphate mixed buffer system at pH 6.1 containing 80 mM KCl (T = 20 ˚C, ν = 50 mV/s). Potentials were measured against an Ag/AgCl reference electrode. Concentrations of protein samples were 150 μM to account for the 40% labeling efficiency of [1] to the protein; control samples of free [1] were measured at 50 μM.

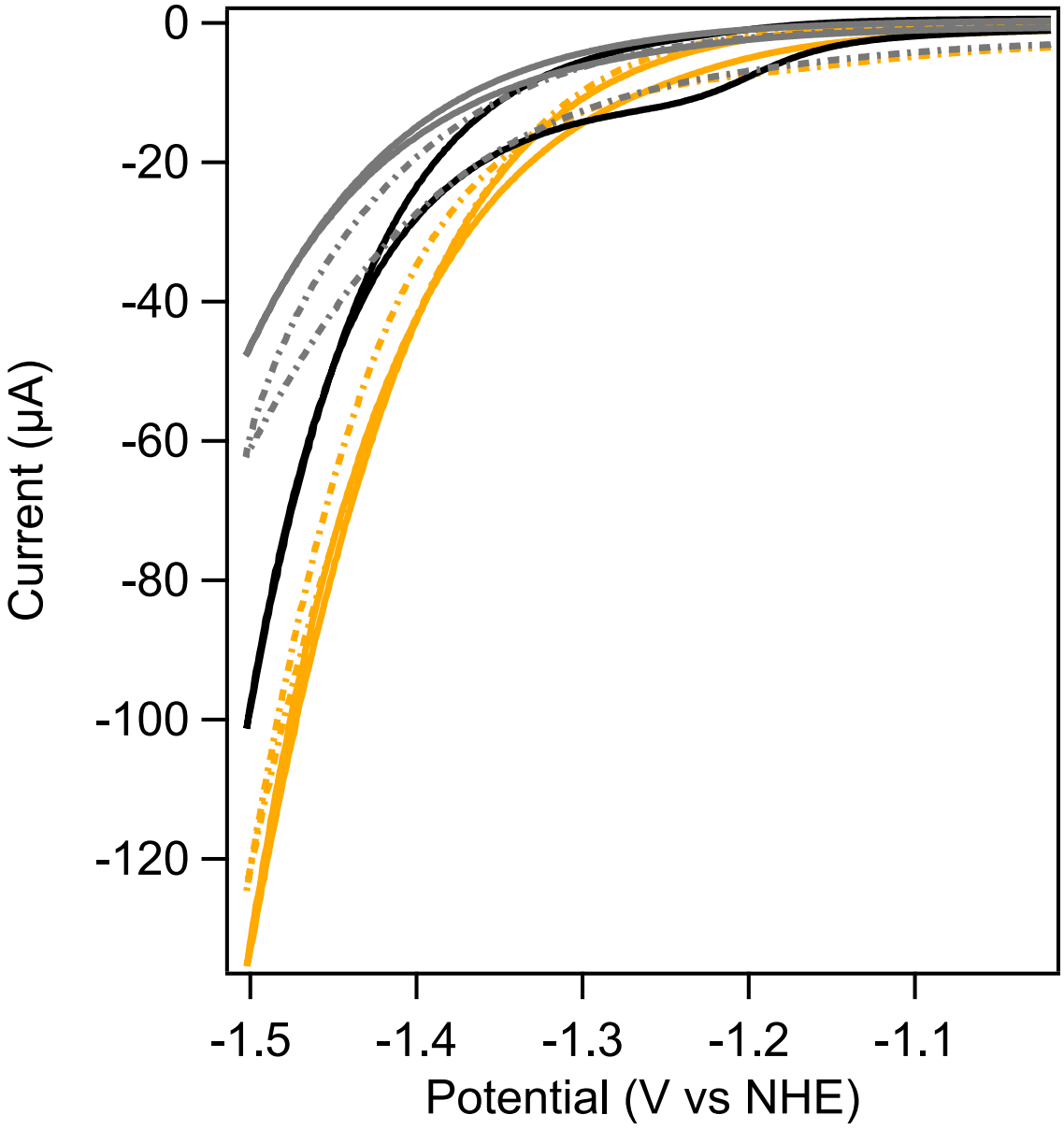

Figure S8. Cyclic voltammograms of WT CuAz-[1] (orange), WT CuAz (gray), and free [1] in solution (black) under CO_2-saturated (solid lines) and inert (dotted lines) atmospheres. Measurements were carried out with a glassy carbon working electrode in a 10 mM CHES, 40 mM phosphate mixed buffer system at pH 6.1 containing 80 mM KCl (T = 20 ˚C, ν = 50 mV/s). Potentials were measured against an Ag/AgCl reference electrode and converted to NHE by the addition of +198 mV. Concentrations of protein samples were 150 µM to account for the 40% labeling efficiency of [1] to the protein; control samples of free [1] were measured at 50 µM.

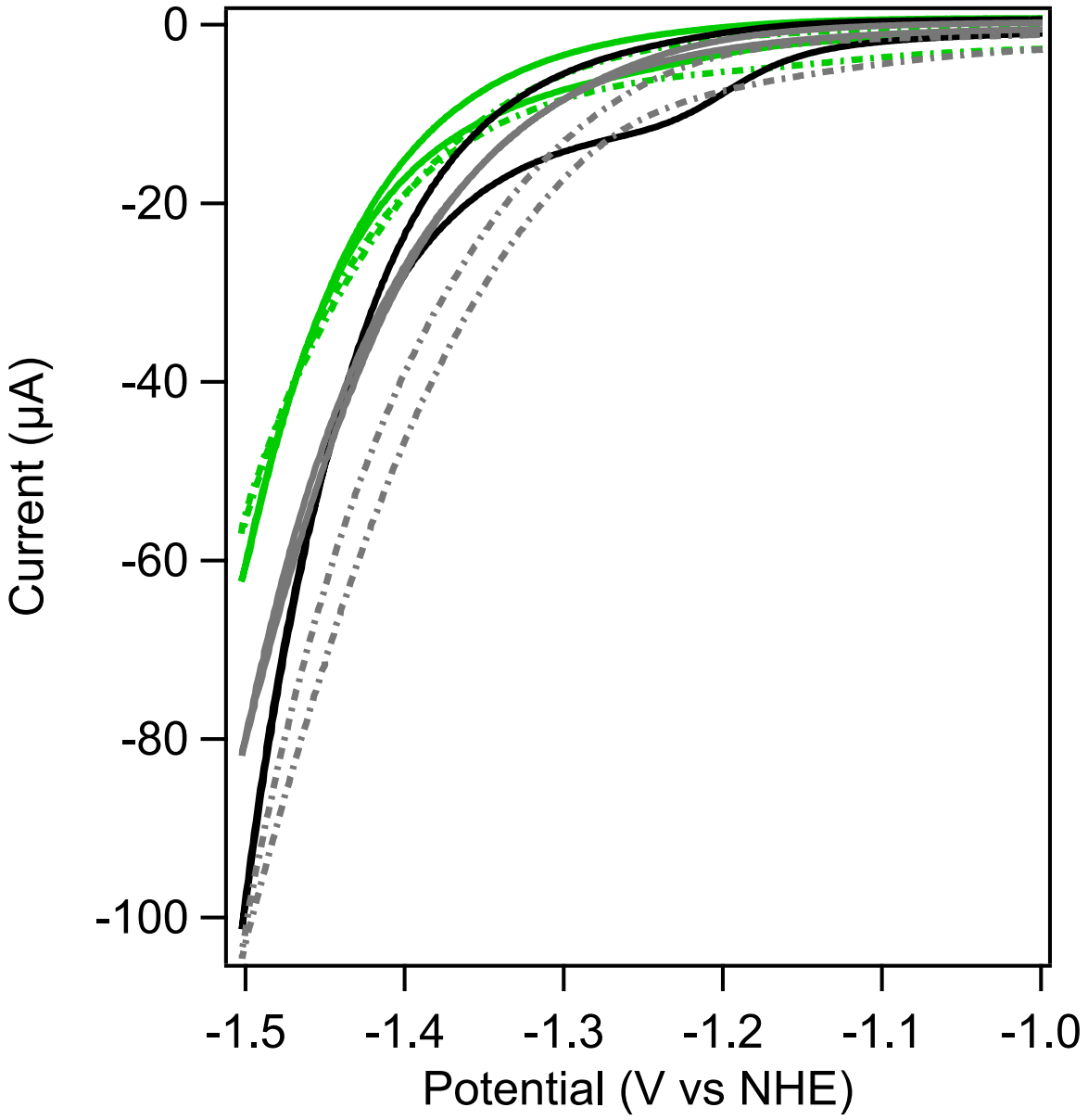

Figure S9. Cyclic voltammograms of H83Q/Q107H ZnAz-[1] (green), H83Q/Q107H ZnAz (gray), and free [1] in solution (black) under CO_2-saturated (solid lines) and inert (dotted lines) atmospheres. Measurements were carried out with a glassy carbon working electrode in a 10 mM CHES, 40 mM phosphate mixed buffer system at pH 6.1 containing 80 mM KCl (T = 20 ˚C, ν = 50 mV/s). Potentials were measured against an Ag/AgCl reference electrode and converted to NHE by the addition of +198 mV. Concentrations of protein samples were 150 μM to account for the 40% labeling efficiency of [1] to the protein; control samples of free [1] were measured at 50 μM.

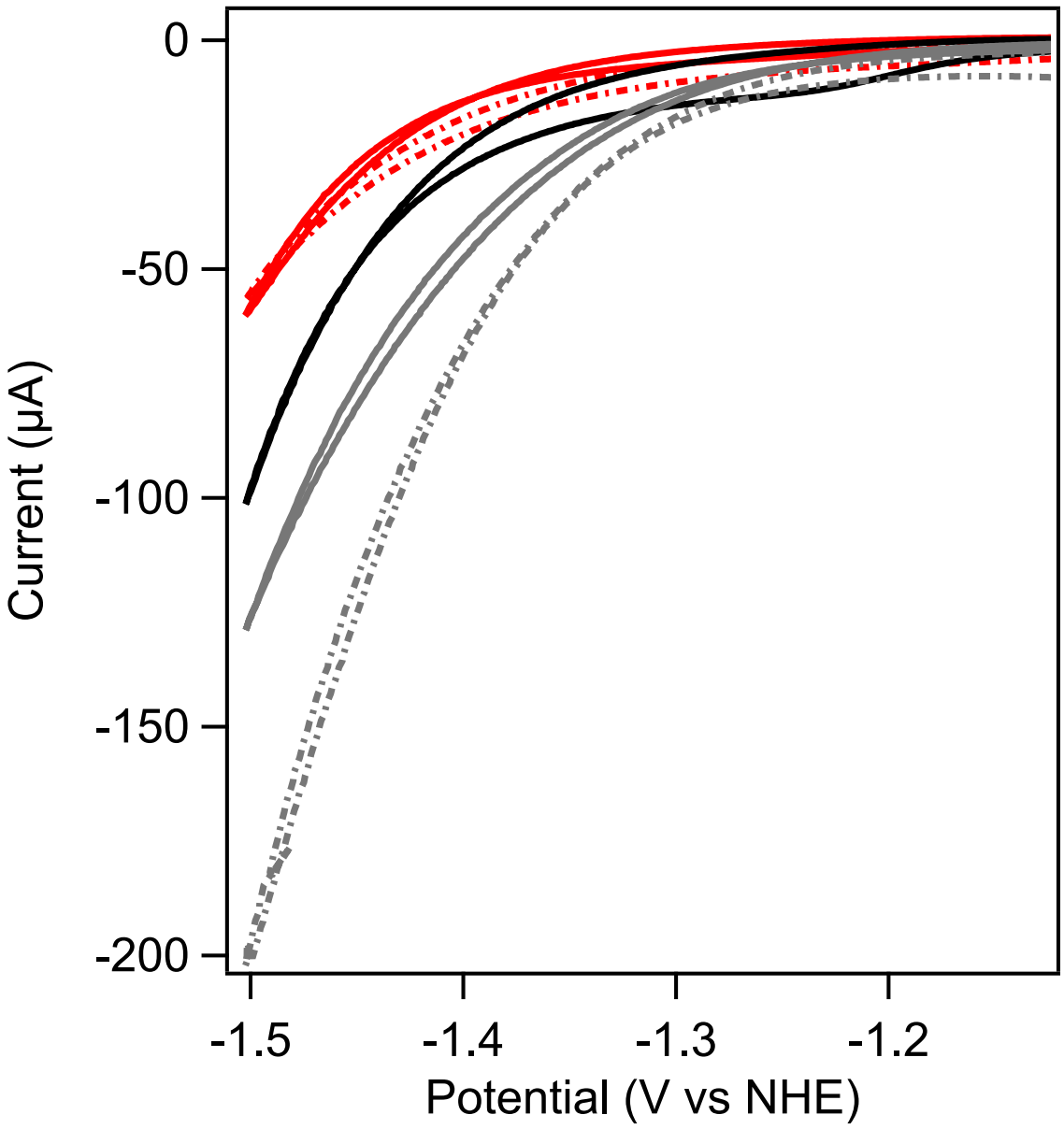

Figure S10. Cyclic voltammograms of WT ZnAz-[1] (red), WT ZnAz (gray), and free [1] in solution (black) under CO_2-saturated (solid lines) and inert (dotted lines) atmospheres. Measurements were carried out with a glassy carbon working electrode in a 10 mM CHES, 40 mM phosphate mixed buffer system at pH 6.1 containing 80 mM KCl (T = 20 ˚C, ν = 50 mV/s). Potentials were measured against an Ag/AgCl reference electrode and converted to NHE by the addition of +198 mV. Concentrations of protein samples were 150 μM to account for the 40% labeling efficiency of [1] to the protein; control samples of free [1] were measured at 50 μM.

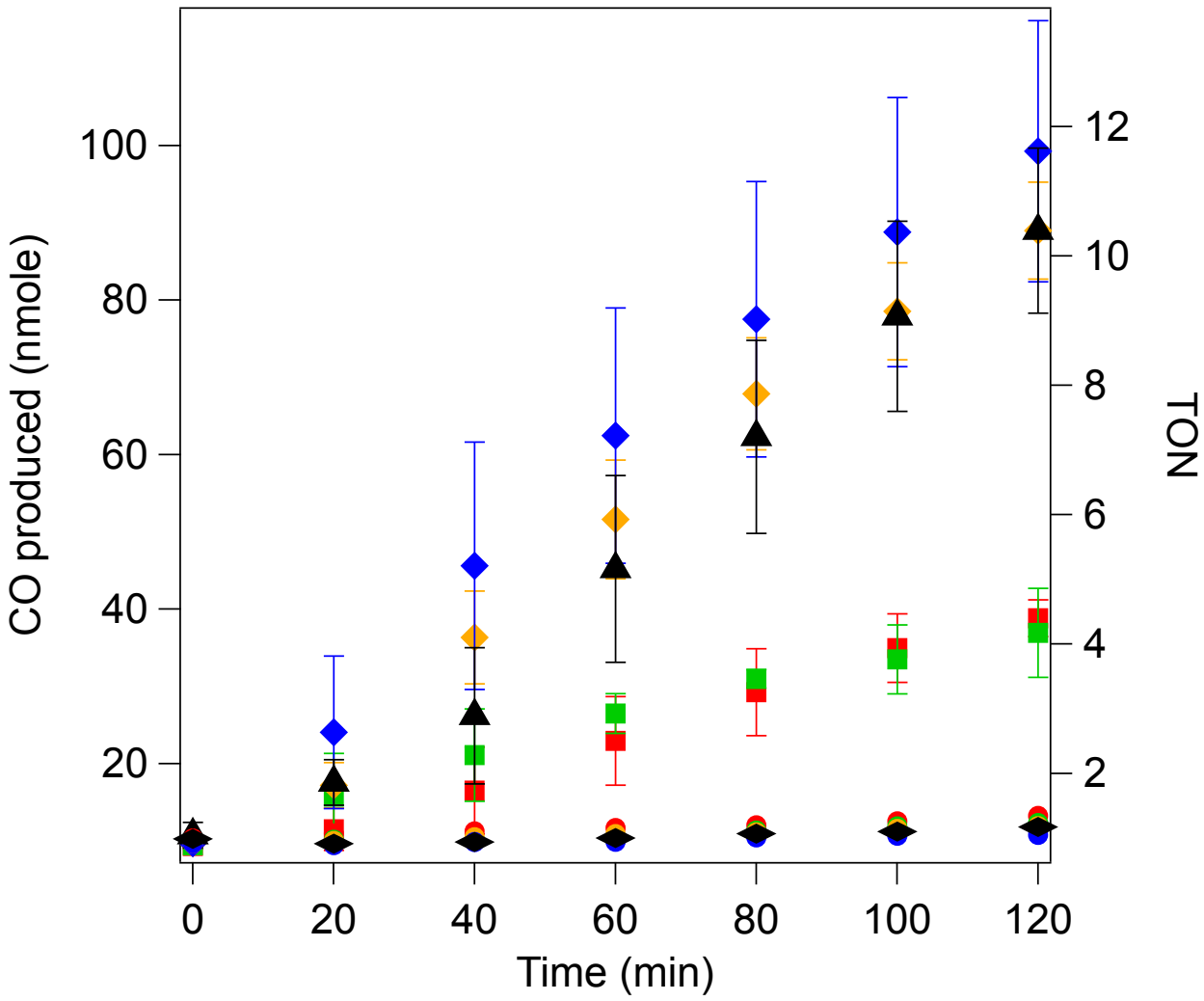

Figure S11. Photoassay results during the first two hours of irradiation showing CO generated by [1]-labeled variants and free [1] in solution (left-hand axis) and turnover numbers (TON, right-hand axis). Data shown represent the average of three trials, with +/- one standard deviation shown as error bars. Circles represent pure protein samples, squares represent labeled Zn derivatives, triangles represent $[Ni^{II}(cyclam)]^{2+}$, and diamonds represent labeled Cu derivatives. Black diamonds represent the catalyst-free control. Color scheme is as follows: H83Q/Q107H CuAz (blue), WT CuAz (orange), H83Q/Q107H ZnAz (green), WT ZnAz (red), and free [1] in solution (black). Concentration of catalyst was 4 μM in a CO_2-saturated buffer mixture containing 1 mM $[Ru^{II}(bpy)_3]^{2+}$ and 100 mM ascorbate in 800 mM phosphate and 10 mM CHES buffer at pH 7.05. TONs on right-hand axis were calculated assuming quantitative labeling.

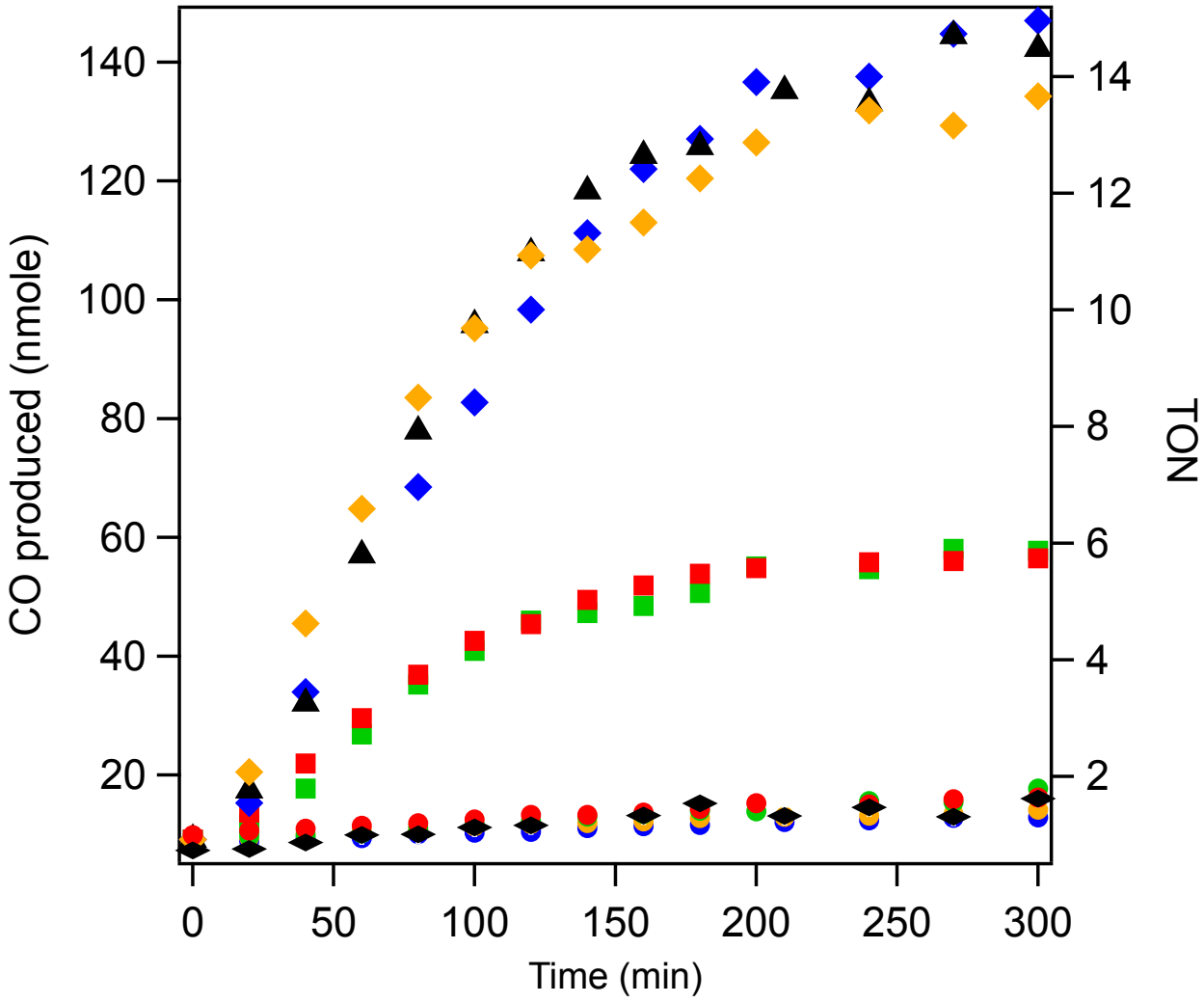

Figure S12. Extended photoassay results over 5 hours of irradiation showing CO generated by [1]-labeled variants and free [1] in solution (left-hand axis) and turnover numbers (TON, right-hand axis). Circles represent pure protein samples, squares represent labeled Zn derivatives, triangles represent $[Ni^{II}(cyclam)]^{2+}$, and diamonds represent labeled Cu derivatives. Black diamonds represent the catalyst-free control. Color scheme is as follows: H83Q/Q107H CuAz (blue), WT CuAz (orange), H83Q/Q107H ZnAz (green), WT ZnAz (red), and free [1] in solution (black). Concentration of catalyst was 4 μM in a CO_2-saturated buffer mixture containing 1 mM $[Ru^{II}(bpy)_3]^{2+}$ and 100 mM ascorbate in 800 mM phosphate and 10 mM CHES buffer at pH 7.05. TONs on right-hand axis were calculated assuming quantitative labeling.

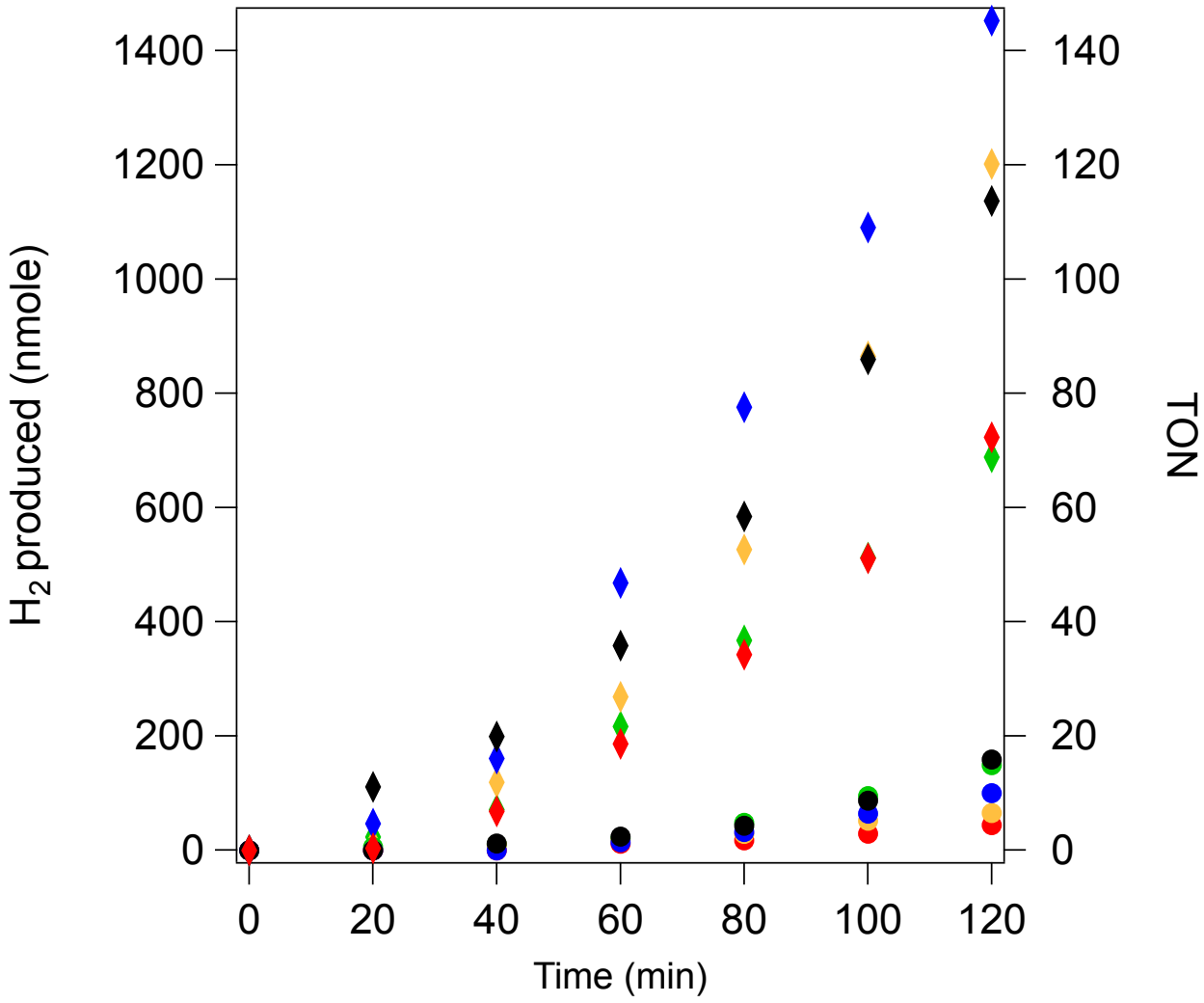

Figure S13. Photoassay results during the first two hours of irradiation showing H_2 generated by [1]-labeled variants and free [1] in solution. Circles represent control samples with pure protein and reaction mixtures lacking [1], and diamonds correspond to labeled variants and free [1] in solution. Color scheme is as follows: H83Q/Q107H CuAz (blue), WT CuAz (orange), H83Q/Q107H ZnAz (green), WT ZnAz (red), and free [1] in solution (black). Concentration of catalyst was 4 μM in a CO_2-saturated buffer mixture containing 1 mM $[Ru^{II}(bpy)_3]^{2+}$ and 100 mM ascorbate in 800 mM phosphate and 10 mM CHES buffer at pH 7.05. TONs on right-hand axis were calculated assuming quantitative labeling. Using this data, measurements of H_2 generated by all catalytic samples were corrected by the subtraction of the corresponding controls.

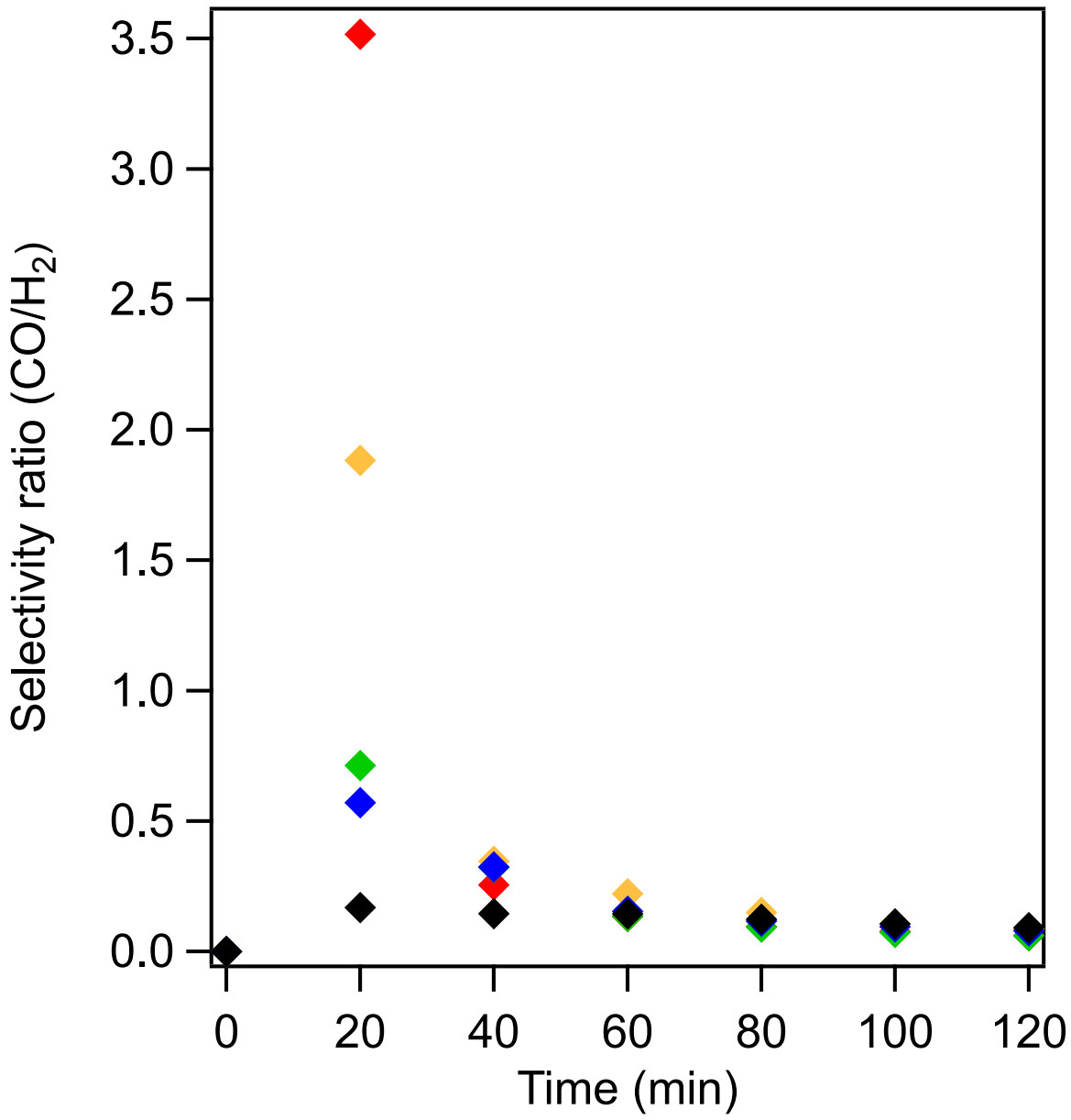

Figure S14. Photocatalytic selectivity for CO generation over H^+ reduction by [1]-labeled Az variants compared to free [1] in solution. Selectivity ratio (SR) is given as moles CO/moles H_2. Color scheme is as follows: H83Q/Q107H CuAz (blue), WT CuAz (orange), H83Q/Q107H ZnAz (green), WT ZnAz (red), and free [1] in solution (black). Concentration of catalyst was 4 μM in a CO_2-saturated buffer mixture containing 1 mM $[Ru^{II}(bpy)_3]^{2+}$ and 100 mM ascorbate in 800 mM phosphate and 10 mM CHES buffer at pH 7.05.

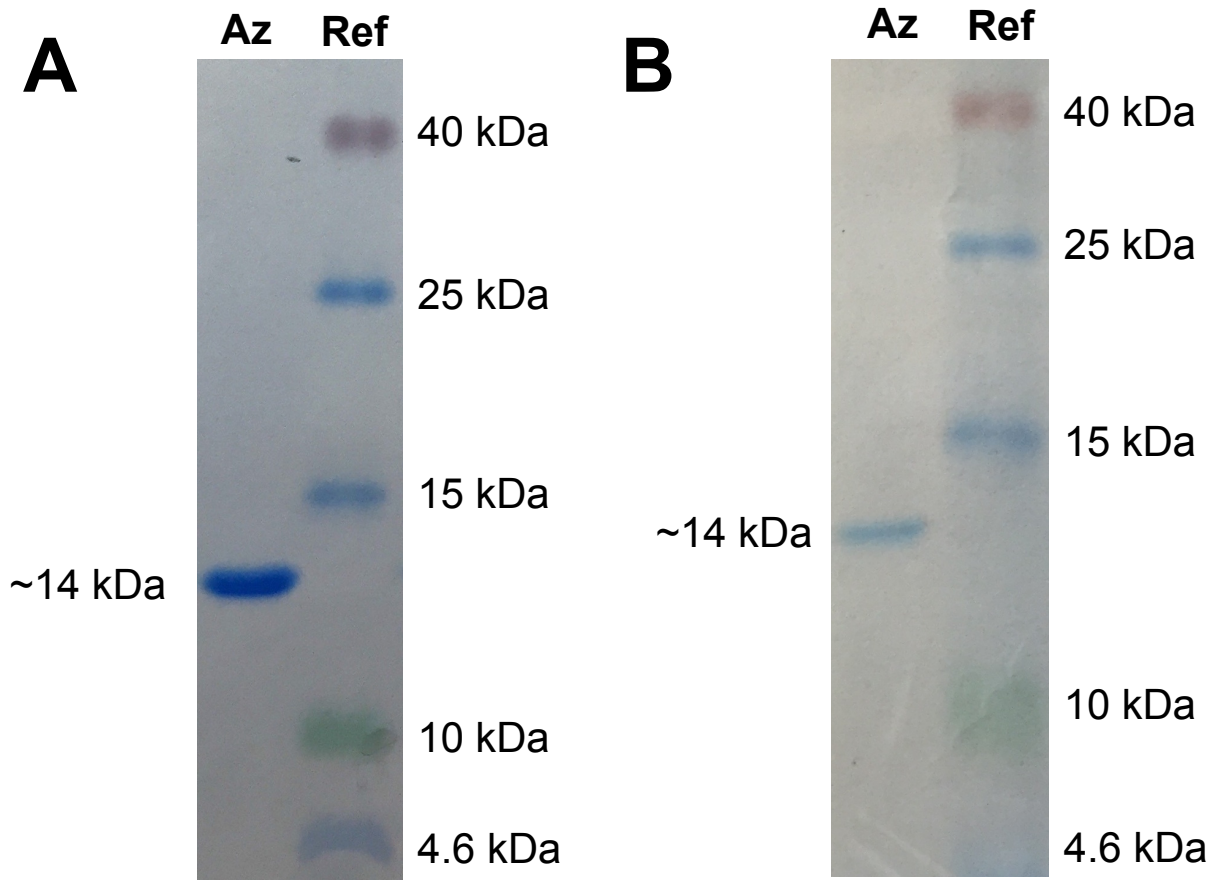

Figure S15. 15% SDS-PAGE of (A) H83Q/Q107H CuAz and (B) WT CuAz referenced against Spectra Multicolor low range protein ladder from Thermo Fisher Scientific.

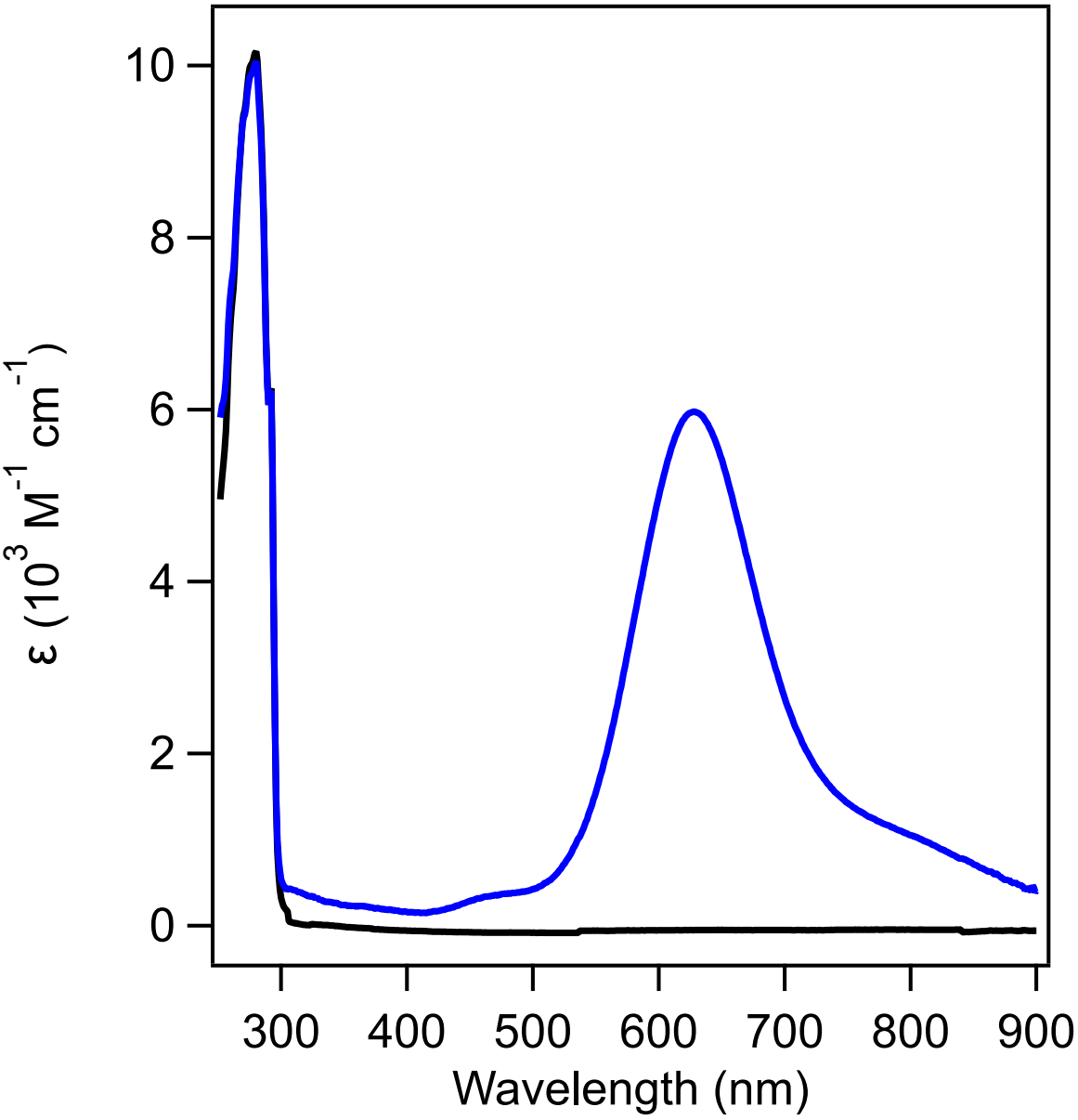

Figure S16. Absorption spectra of H83Q/Q107H derivatives. H83Q/Q107H CuAz (blue) and H83Q/Q107H ZnAz (black) in 50 mM CHES, pH 9.0.

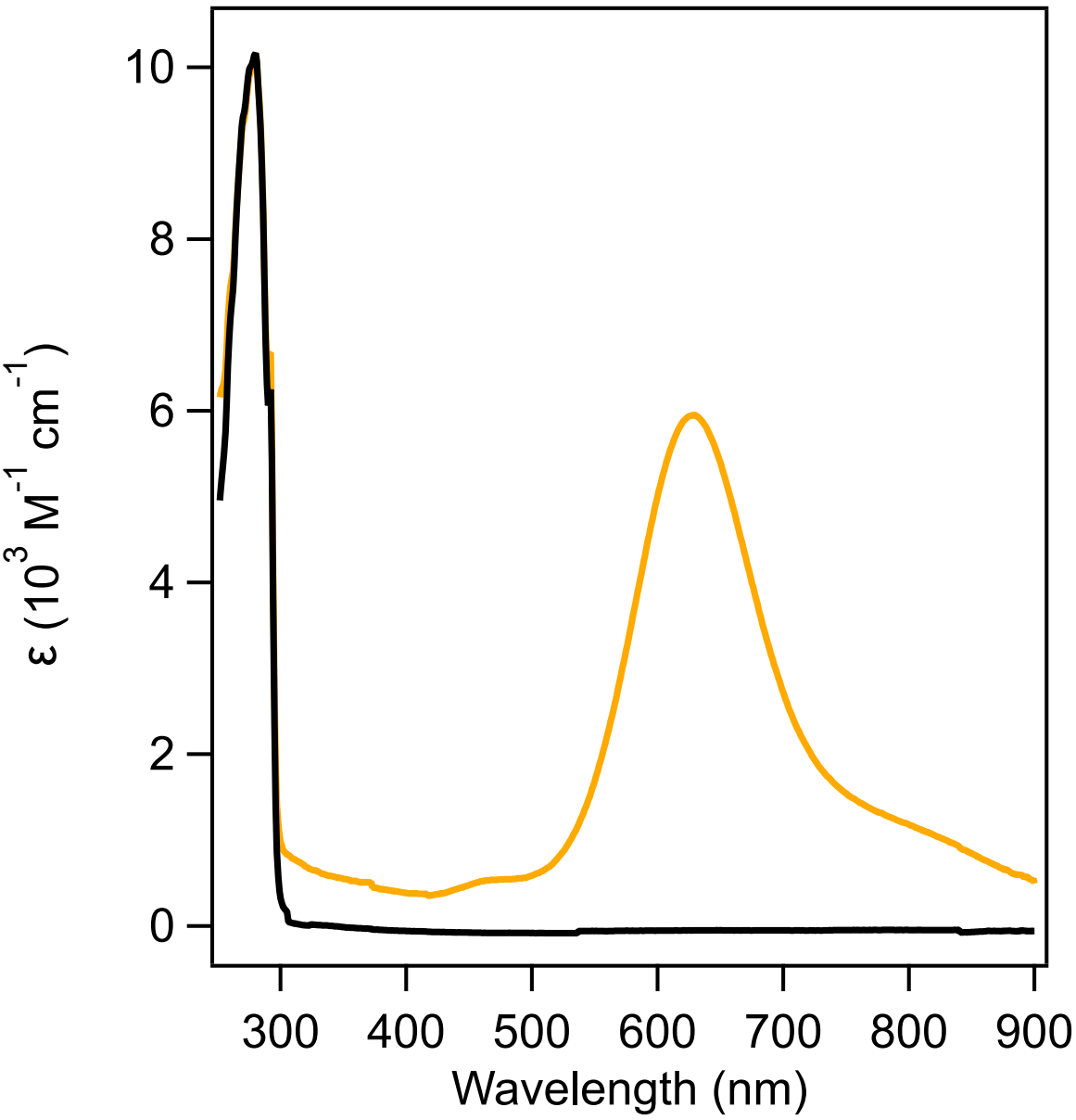

Figure S17. Absorption spectra of WT derivatives. WT CuAz (orange) and WT ZnAz (black) in 50 mM CHES, pH 9.0.

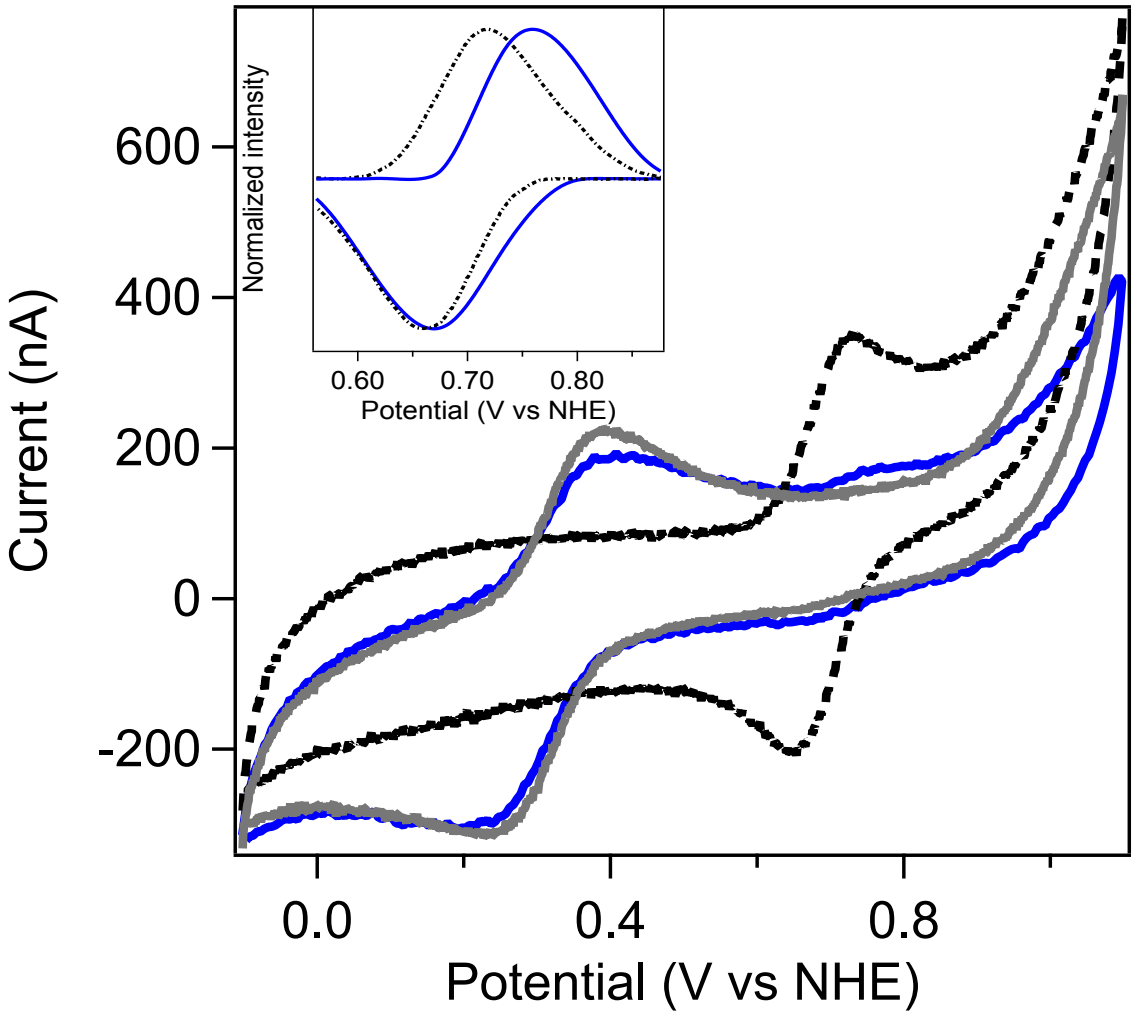

Figure S18. Cyclic voltammograms of H83Q/Q107H CuAz-[1] (blue), H83Q/Q107H CuAz (gray), and free [1] in solution (black) under a CO_2–saturated atmosphere. Measurements were carried out with a glassy carbon working electrode in a 10 mM CHES, 40 mM phosphate mixed buffer system at pH 6.1 containing 80 mM KCl (T = 20 ˚C, ν = 10 mV/s). Potentials were measured against an Ag/AgCl reference electrode and converted to NHE by the addition of +198 mV. Concentrations of protein samples were 150 μM; control samples of free [1] were measured at 50 μM. (*Inset*) Baseline-corrected CV data showing the $Ni^{III/II}$ one-electron couple. Baseline subtractions were performed using the QSOAS program.

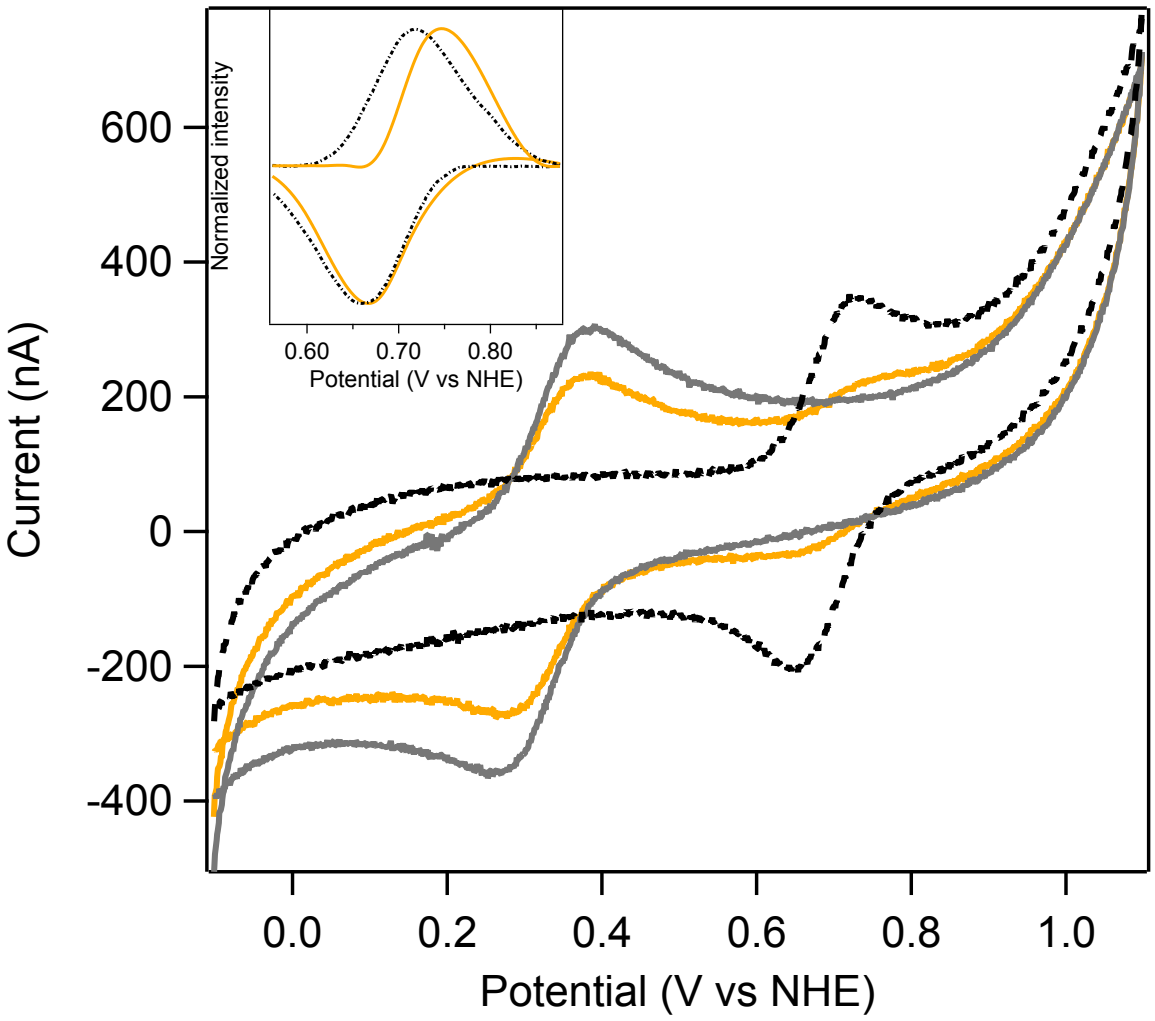

Figure S19. Cyclic voltammograms of WT CuAz-[1] (orange), WT CuAz (gray), and free [1] in solution (black) under a CO_2–saturated atmosphere. Measurements were carried out with a glassy carbon working electrode in a 10 mM CHES, 40 mM phosphate mixed buffer system at pH 6.1 containing 80 mM KCl (T = 20 ˚C, ν = 10 mV/s). Potentials were measured against an Ag/AgCl reference electrode and converted to NHE by the addition of +198 mV. Concentrations of protein samples were 150 μM; control samples of free [1] were measured at 50 μM. (*Inset*) Baseline-corrected CV data showing the $Ni^{III/II}$ one-electron couple. Baseline subtractions were performed using the QSOAS program.

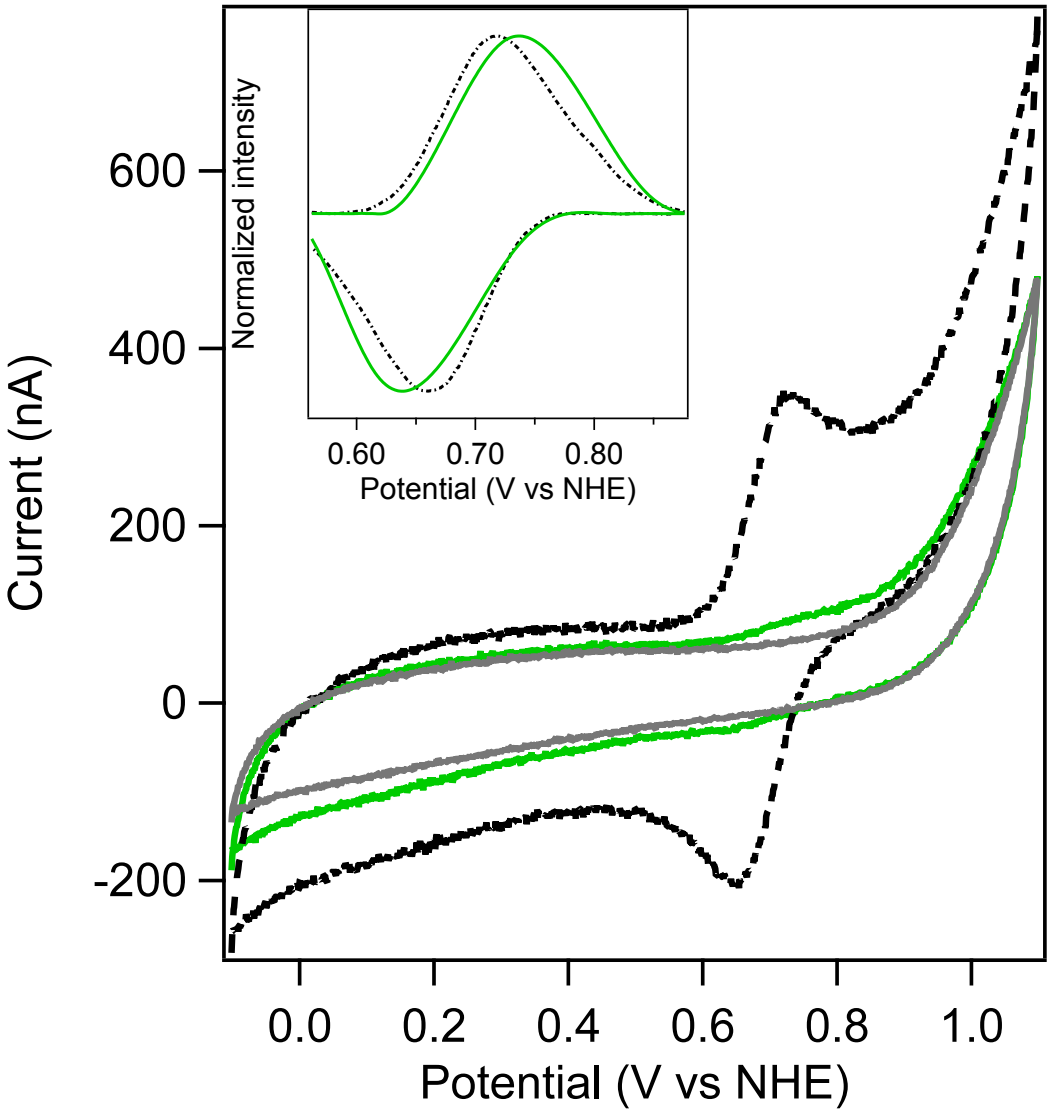

Figure S20. Cyclic voltammograms of H83Q/Q107H ZnAz-[1] (green), H83Q/Q107H CuAz (gray), and free [1] in solution (black) under a CO_2–saturated atmosphere. Measurements were carried out with a glassy carbon working electrode in a 10 mM CHES, 40 mM phosphate mixed buffer system at pH 6.1 containing 80 mM KCl (T = 20 ˚C, ν = 10 mV/s). Potentials were measured against an Ag/AgCl reference electrode and converted to NHE by the addition of +198 mV. Concentrations of protein samples were 150 μM; control samples of free [1] were measured at 50 μM. (*Inset*) Baseline-corrected CV data showing the $Ni^{III/II}$ one-electron couple. Baseline subtractions were performed using the QSOAS program.

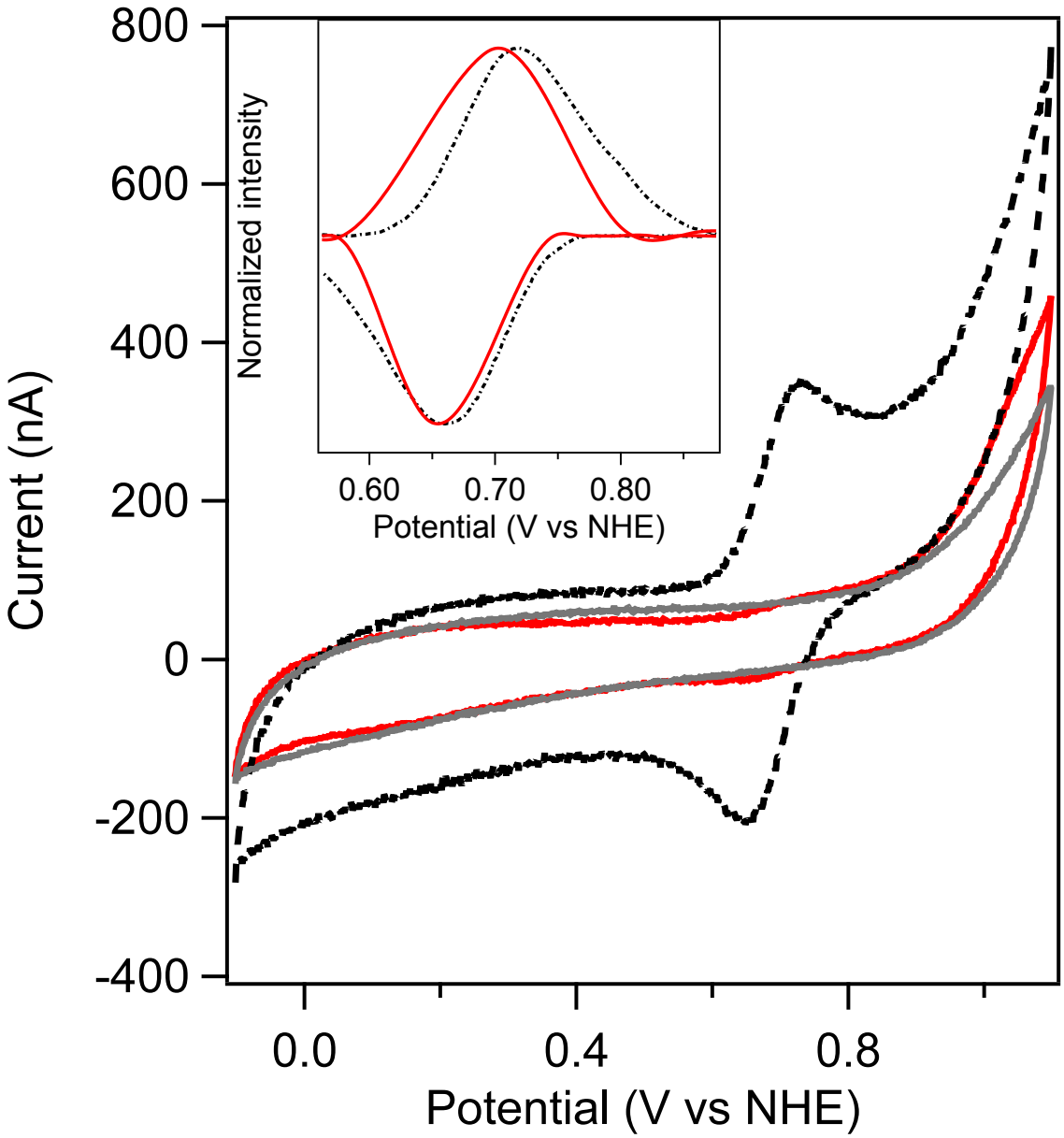

Figure S21. Cyclic voltammograms of WT ZnAz-[1] (red), WT ZnAz (gray), and free [1] in solution (black) under a CO_2–saturated atmosphere. Measurements were carried out with a glassy carbon working electrode in a 10 mM CHES, 40 mM phosphate mixed buffer system at pH 6.1 containing 80 mM KCl (T = 20 ˚C, ν = 10 mV/s). Potentials were measured against an Ag/AgCl reference electrode and converted to NHE by the addition of +198 mV. Concentrations of protein samples were 150 μM; control samples of free [1] were measured at 50 μM. (*Inset*) Baseline-corrected CV data showing the $Ni^{III/II}$ one-electron couple. Baseline subtractions were performed using the QSOAS program.

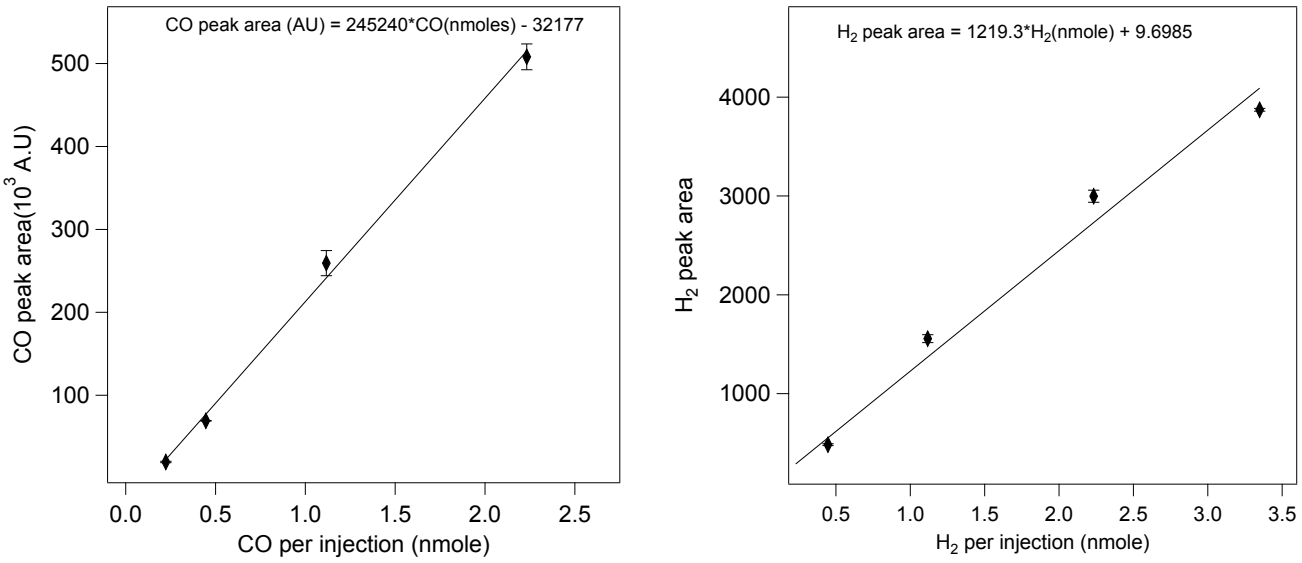

Figure S22. Calibration curves used for CO and H_2 quantification. Curves were prepared using variable-volume injections of a mixed-gas calibration standard from Scotty Gases.

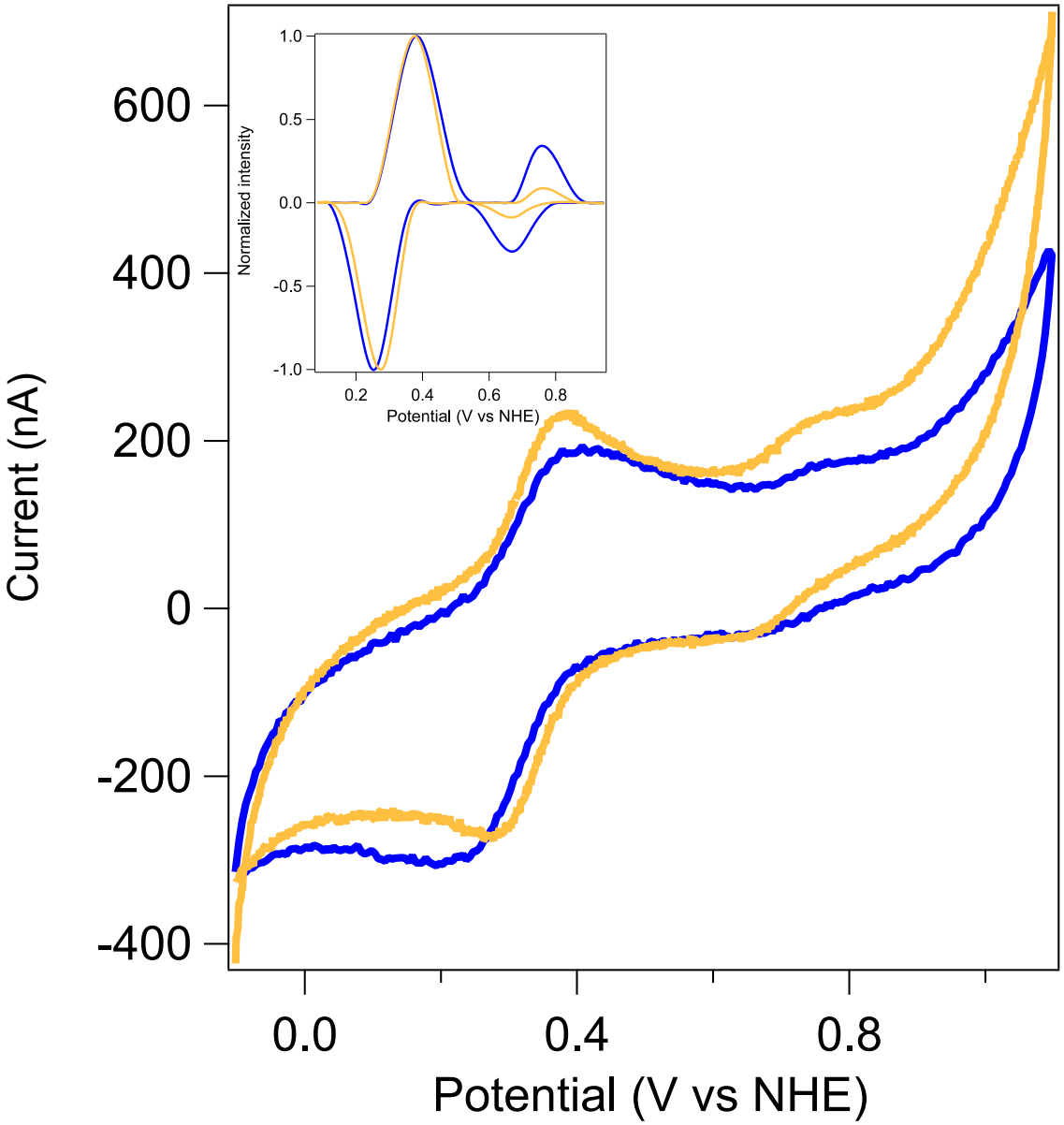

Figure S23. CV data of H83Q/Q107H CuAz-[1] (blue) and WT CuAz-[1] (orange). Measurements carried out as described in Figure S5. Integrated intensities of the one-electron $Ni^{III/II}$ couples show approximately 30-40% of the integrated areas of the $Cu^{II/I}$ couple, comparable to the estimated 40% labeling efficiencies obtained using the absorption spectra of the ZnAz-[1] variants. While diffusion limitations complicate quantitative use of these areas, the similarity between the electrochemical and spectroscopic estimates further justifies the assumption that comparable labeling efficiencies were achieved for both Zn- and Cu-substituted proteins.

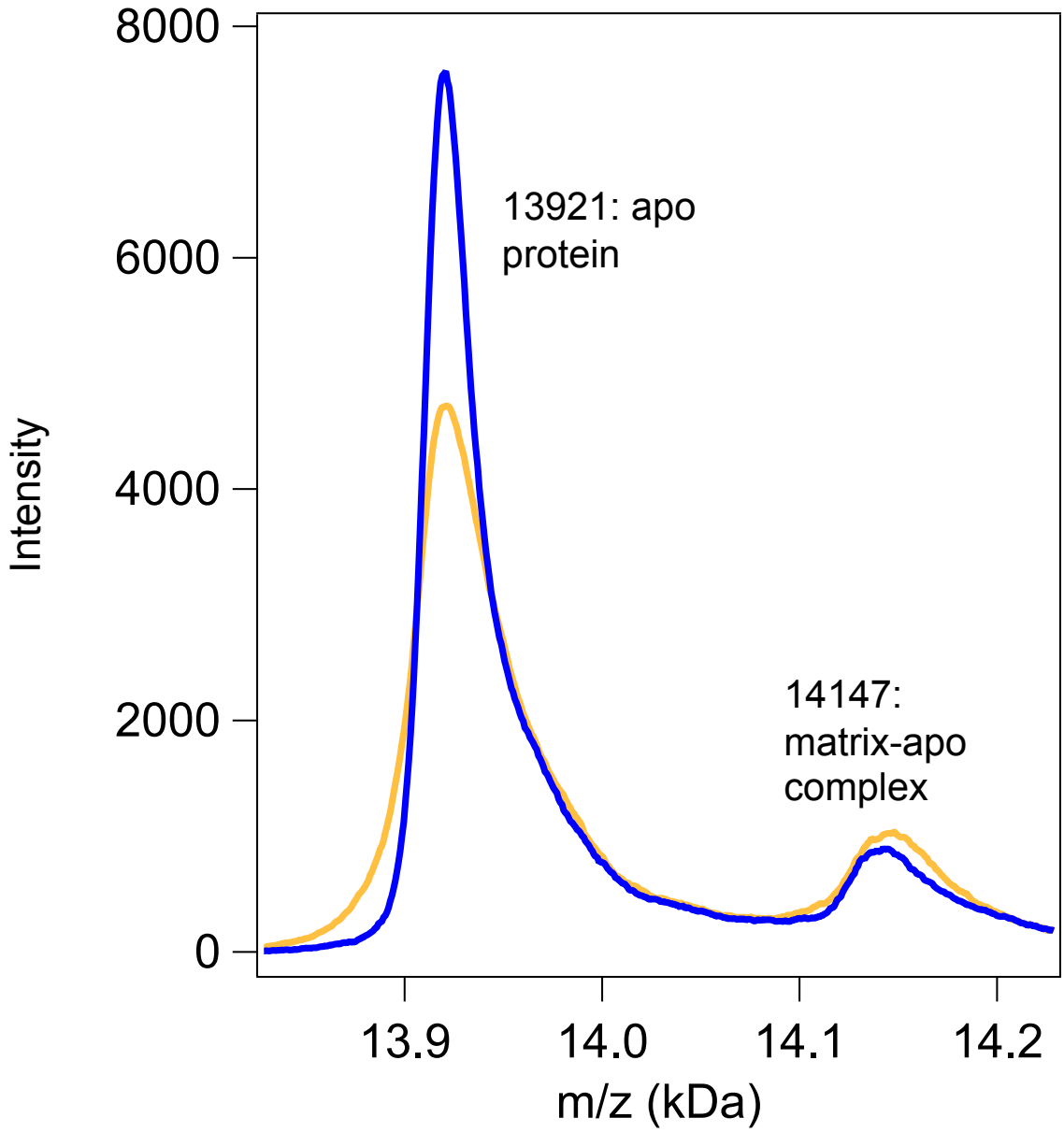

Figure S24. MALDI-TOF data of H83Q/Q107H CuAz (blue) and WT CuAz (orange). A final protein concentration of 10 μM protein was used for analysis on a Bruker microFlex MALDI-TOF spectrometer. Samples were mixed 1:1 with a matrix composed of 200 mM sinapic acid, 30 mM ammonium citrate in 30% acetonitrile.

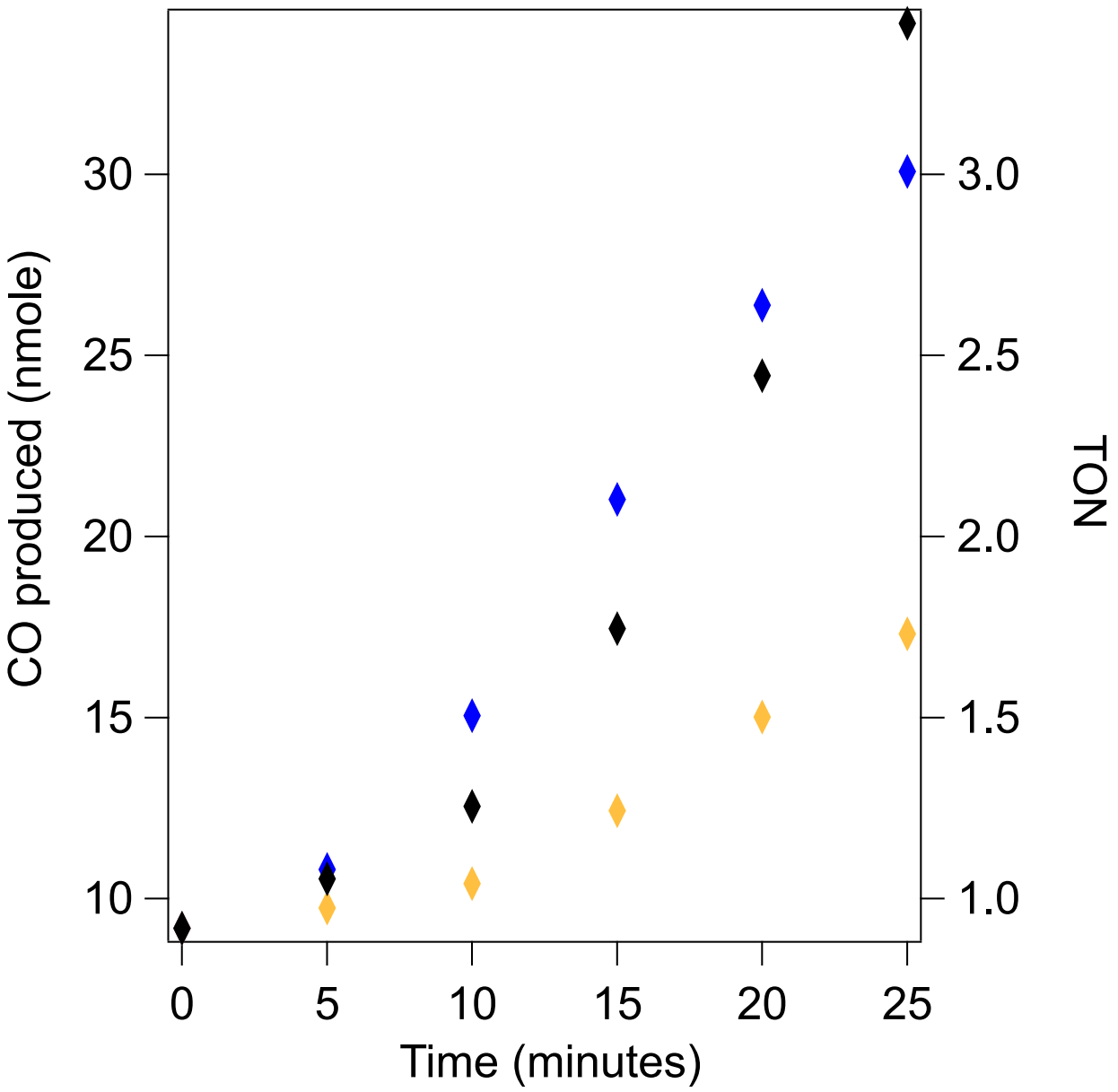

Figure S25. Photoinduced CO_2 reduction by H83Q/Q107H CuAz (blue), WT CuAz (orange), and free [1] in solution (black) during the first 20 minutes of irradiation. Concentration of catalyst was 4 μM in a CO_2-saturated buffer mixture containing 1 mM $[Ru^{II}(bpy)_3]^{2+}$ and 100 mM ascorbate in 800 mM phosphate and 10 mM CHES buffer at pH 7.05. TONs on right-hand axis were calculated assuming quantitative labeling.

References

(1) Manesis, A. C.; Shafaat, H. S. *Inorg. Chem.* **2015**, *54* (16), 7959–7967.
(2) Hutnik, C. M.; Szabo, A. G. *Biochemistry* **1989**, *28* (9), 3923–3934.
(3) Larson, B. C.; Pomponio, J. R.; Shafaat, H. S.; Kim, R. H.; Leigh, B. S.; Tauber, M. J.; Kim, J. E. *J. Phys. Chem. B* **2015**, 150217092731004.
(4) Shafaat, H. S.; Leigh, B. S.; Tauber, M. J.; Kim, J. E. *J. Am. Chem. Soc.* **2010**, *132* (26), 9030–9039.
(5) Bosnich, B.; Poon, C. K.; Tobe, M. L. *Inorg. Chem.* **1965**, *4* (8), 1102–1108.
(6) Fourmond, V.; Hoke, K.; Heering, H. A.; Baffert, C.; Leroux, F.; Bertrand, P.; Léger, C. *Bioelectrochemistry* **2009**, *76* (1-2), 141–147.
(7) Sommer, D. J.; Vaughn, M. D.; Ghirlanda, G. *Chem Commun* **2014**, *50* (100), 15852–15855.